

Article

A Structure-Activity Relationship Study of Bitopic N6-Substituted Adenosine Derivatives as Biased Adenosine A1 Receptor Agonists

Luigi Aurelio, Jo-Anne Baltos, Leigh Ford, Anh T.N. Nguyen, Manuela Jörg, Shane M. Devine, Celine Valant, Paul J. White, Arthur Christopoulos, Lauren T. May, and Peter J. Scammells

J. Med. Chem., **Just Accepted Manuscript** • DOI: 10.1021/acs.jmedchem.8b00047 • Publication Date (Web): 15 Feb 2018

Downloaded from <http://pubs.acs.org> on February 16, 2018

Just Accepted

"Just Accepted" manuscripts have been peer-reviewed and accepted for publication. They are posted online prior to technical editing, formatting for publication and author proofing. The American Chemical Society provides "Just Accepted" as a service to the research community to expedite the dissemination of scientific material as soon as possible after acceptance. "Just Accepted" manuscripts appear in full in PDF format accompanied by an HTML abstract. "Just Accepted" manuscripts have been fully peer reviewed, but should not be considered the official version of record. They are citable by the Digital Object Identifier (DOI®). "Just Accepted" is an optional service offered to authors. Therefore, the "Just Accepted" Web site may not include all articles that will be published in the journal. After a manuscript is technically edited and formatted, it will be removed from the "Just Accepted" Web site and published as an ASAP article. Note that technical editing may introduce minor changes to the manuscript text and/or graphics which could affect content, and all legal disclaimers and ethical guidelines that apply to the journal pertain. ACS cannot be held responsible for errors or consequences arising from the use of information contained in these "Just Accepted" manuscripts.



ACS Publications

A Structure-Activity Relationship Study of Bitopic N^6 -Substituted Adenosine Derivatives as Biased Adenosine A_1 Receptor Agonists

Luigi Aurelio,^{†,§} Jo-Anne Baltos,^{‡,§} Leigh Ford,[†] Anh T. N. Nguyen,[‡] Manuela Jörg,[†]
Shane M. Devine,[†] Celine Valant,[‡] Paul J. White,[‡] Arthur Christopoulos,[‡]
Lauren T. May,^{‡,*} Peter J. Scammells^{†,*}

[†] *Medicinal Chemistry, Monash Institute of Pharmaceutical Sciences; Monash University, Parkville, VIC 3052, Australia*

[‡] *Drug Discovery Biology, Monash Institute of Pharmaceutical Sciences & Department of Pharmacology, Monash University, Parkville, VIC 3052, Australia*

[§] These authors contributed equally to this manuscript

ABSTRACT: The adenosine A_1 receptor (A_1AR) is a potential novel therapeutic target for myocardial ischemia-reperfusion injury. However, to date, clinical translation of prototypical A_1AR agonists has been hindered due to dose limiting adverse effects. Recently, we demonstrated that the biased bitopic agonist **1**, consisting of an adenosine pharmacophore linked to an allosteric moiety, could stimulate cardioprotective A_1AR signalling in the absence of unwanted bradycardia. Therefore, this study aimed to investigate the structure-activity relationship of compound **1** biased agonism. A series of novel derivatives of **1** were synthesised and pharmacologically profiled. Modifications were made to the orthosteric adenosine pharmacophore, linker and allosteric 2-amino-3-benzoylthiophene pharmacophore to probe the structure-activity relationships, particularly in terms of biased signalling, as well as A_1AR activity and subtype selectivity. Collectively, our findings demonstrate that the allosteric moiety, particularly the 4-(trifluoromethyl)phenyl substituent of the thiophene scaffold, is important in conferring bitopic ligand bias at the A_1AR .

■ INTRODUCTION

The adenosine receptor family consists of four subtypes, namely the A₁AR, A_{2A}AR, A_{2B}AR and A₃AR, which are part of the G protein-coupled receptor (GPCR) superfamily.^{1,2} The A₁AR is an important therapeutic target,³⁻⁶ known to stimulate protective effects in heart tissue, particularly in models of ischemia-reperfusion injury (IRI).^{7,8} However, there is a high attrition rate in the transition of A₁AR agonists into clinic due to dose limiting side effects such as hypotension, bradycardia and atrioventricular block.⁹⁻¹¹ Therefore, the primary obstacle is that both the therapeutic and adverse effects are mediated by the A₁AR.^{12,13} In contrast to prototypical A₁AR subtype selective agonists, A₁AR biased agonists have the potential to overcome these commonly observed limitations. Biased agonists can stimulate distinct signalling profiles to that of prototypical agonists through stabilizing a different spectrum of receptor conformations.¹⁴⁻¹⁶ As such, GPCR biased agonism provides the opportunity to design compounds that selectively stimulate the pathway associated with the therapeutic effect, whilst avoiding signalling associated with on-target adverse effects.

Our group has previously reported the identification of VCP746 (**1**) (Figure 1), a rationally designed adenosine receptor bivalent ligand that has a bitopic mechanism of action and biased profile at the A₁AR.¹³ Bitopic ligands are bivalent molecules that interact simultaneously with an orthosteric site and allosteric binding site within a GPCR monomer.^{17,18} Compound **1** consists of the orthosteric agonist adenosine and a biased allosteric thiophene pharmacophore, which are tethered together by an aromatic linker unit and a 6-carbon alkyl linker (Figure 1). Pharmacological evaluation of **1** revealed significant bias away from calcium mobilization, compared to ERK1/2 phosphorylation, Akt phosphorylation and inhibition of cAMP accumulation, relative to the reference agonist NECA.¹⁹ Furthermore, we were able to demonstrate the compounds ability to protect against ischemia in native A₁AR-expressing cardiomyoblasts without effects on the rat atrial heart rate.¹³ In summary, our proof of concept studies have shown a link between the biased pharmacological profile of compound **1** to its ability to promote on-target efficacy without on-target

adverse effects. This work embodied an important step in the quest of rationally identifying better drugs that act at the A₁AR.

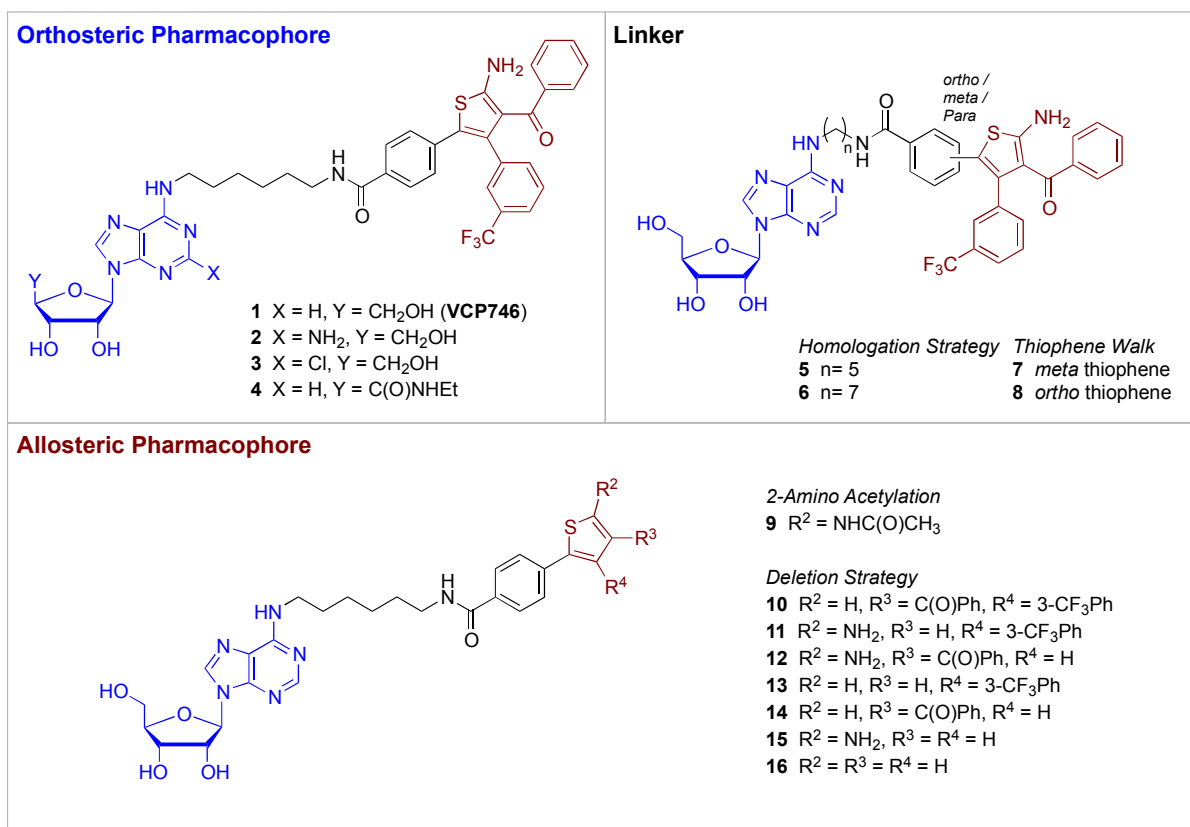


Figure 1. Chemical structure of the biased bitopic A₁AR ligand **1** and an overview of the structural changes made as part of the SAR study. The colours represent the different components of the bitopic ligand; namely, the orthosteric pharmacophore (blue), linker (black) and the allosteric pharmacophore (red).

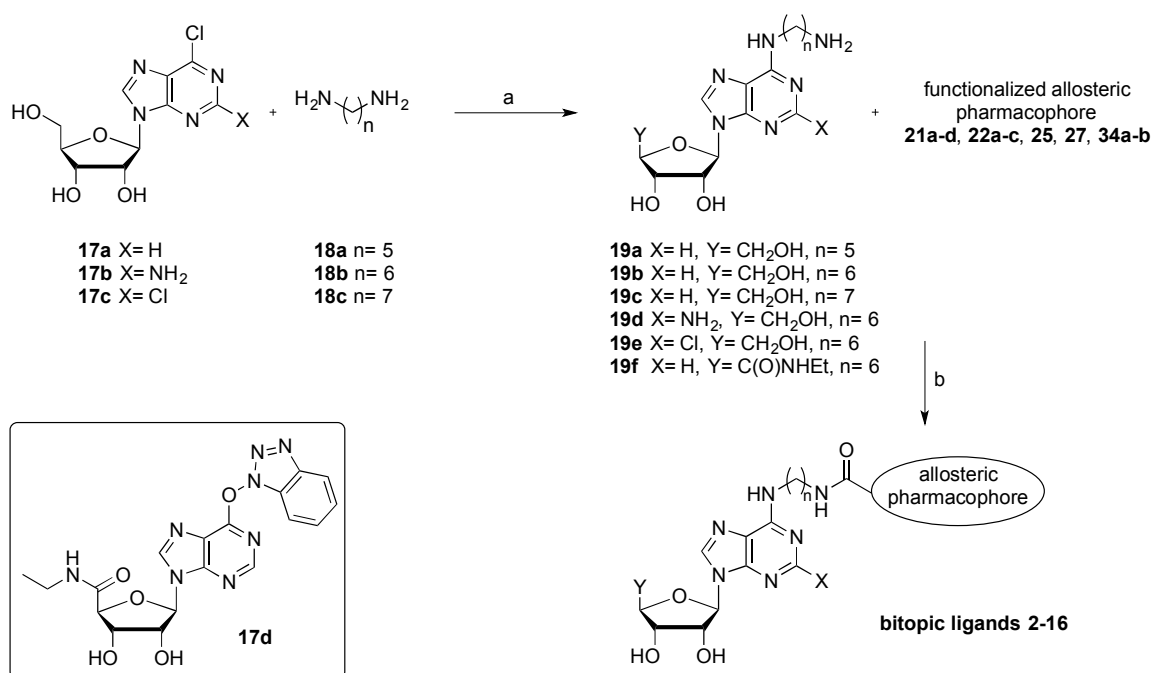
The aim of the current study was to understand the structure-activity relationships underlying the physiologically relevant A₁AR biased agonism mediated by compound **1**. Herein, we describe the synthesis and pharmacological evaluation of a series of compounds that derived from **1**. We have made structural changes to the orthosteric pharmacophore (**2–4**), the linker (**5–8**) and the allosteric pharmacophore (**9–16**) (Figure 1). Modification to the 2-position of the purine scaffold and the 5'-position of the sugar moiety have been shown to affect the subtype selectivity of adenosine agonists. Therefore, we synthesized the 2-amino (**2**) and 2-chloro (**3**) substituted analogs

of **1** as well as the 5'-ethylcarboxamide derivative (**4**). The linker has been modified to probe the effects of subtle changes in length (i.e. one fewer or one additional methylene unit, **5** and **6** respectively) as well as its point of attachment to the thiophene (*meta* / *ortho*, **7** and **8** respectively). Finally, the allosteric moiety has been altered either by acetylation of the amino group (**9**) or a deletion strategy removing one (**10-12**), two (**13-15**) or all three substituents (**16**) of the thiophene ring.

RESULTS AND DISCUSSION

Chemistry. The synthetic pathway used for the preparation of the bitopic analogs was based on the general approach shown in Scheme 1. First, the respective orthosteric pharmacophore (**17a-d**) was functionalized with the diaminoalkyl spacer (**18a-c**), which then was coupled with the respective carboxylic acid functionalized allosteric portion under standard coupling conditions to obtain the final bitopic analogs (**1-16**).

Scheme 1. Synthesis of the bitopic adenosine A₁ receptor agonists^a



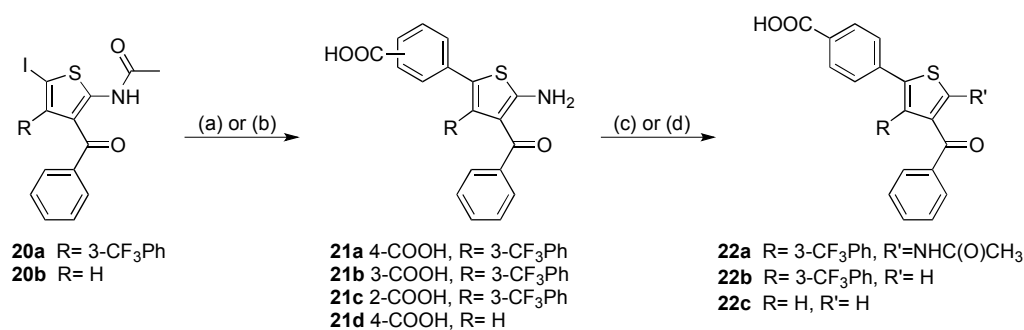
^aReagents and conditions: (a) (i) Et₃N, EtOH, reflux, 18-92% for **19a-e**; (ii) diaminoalkane (**18b**), Et₃N, EtOH, rt, product not isolated for **19f**; (b) BOP, Et₃N, DMF, rt, 6-90%.

Therefore, the respective diaminoalkanes (**18a–c**) were introduced via a substitution reaction with the 6-chloropurine riboside derivatives **17a–c** in ethanol and triethylamine. The reactions were stirred at reflux until complete conversion was observed, upon cooling to room temperature the resultant precipitate was filtered to give intermediates **19a–d** in good yields (54–92%); with the exception of **19e** which was obtained as a light yellowish oil in only 18% yield. Intermediate **19f** was synthesized using the same conditions but at room temperature and starting from (2*S*,3*S*,4*R*,5*R*)-5-(6-((1*H*-benzo[*d*][1,2,3]triazol-1-yl)oxy)-9*H*-purin-9-yl)-*N*-ethyl-3,4-dihydroxytetrahydrofuran-2-carboxamide (**17d**), which was prepared from the commercially available inosine using a six-step synthetic route based on reported methods in the literature (see Supporting Information).^{20–22}

The final bitopic ligands **2–16** were obtained by linking the orthosteric amine intermediates **19a–f** and the prior prepared carboxylic acid functionalized allosteric moieties **21a–d**, **22a–c**, **25**, **27** and **34a–b** (Scheme 2–4). The formation of the amide bond was achieved using standard peptide coupling conditions and afforded the bitopic ligands **2–16** in yields ranging between 6–90%.

The functionalized carboxylic acid allosteric moieties were synthesized via the routes illustrated in Schemes 2–4. We have previously published the synthesis of the iodothiophenes **20** (Scheme 2), which can be achieved via either a two-step or one-pot microwave-assisted Gewald procedure starting from the respective benzoylacetone nitrile and acetophenone,^{23,24} followed by the acetylation of the amino group and iodination in the 5-position.¹³ The carboxylic acid functionalized allosteric moieties **21a–d** were afforded in good yields by a Suzuki-coupling reaction with **20a** or **20b** and the respective *ortho*, *meta* or *para*-substituted methoxycarbonylphenyl boronic acids, followed by the simultaneous hydrolysis of the ester and deacetylation under alkaline conditions. Acetylation of **21a** with acetic anhydride gave the diacetylated intermediate (*O*- and *N*-acetylation), which was treated with lithium hydroxide to afford **22a** in 98% yield. Alternatively, **21a** and **21d** were treated with *t*-butylnitrite in DMF at 65 °C to remove the amino group and provide compounds **22b** and **22c** in 91% and 71% yield, respectively.

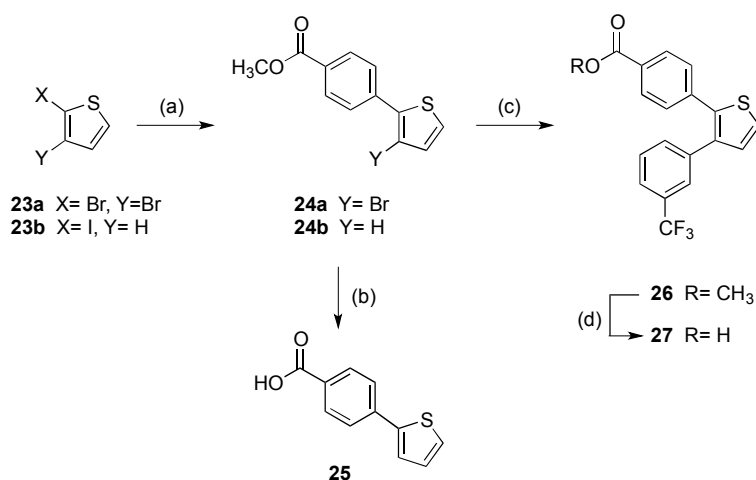
Scheme 2. Synthesis of the functionalized allosteric A₁AR pharmacophores **20a-d and **22a-c**^a**



^aReagents and conditions: (a) 3- or 4-methoxycarbonylphenyl boronic acid, Pd(PPh₃)₂Cl₂, 2 M K₃PO₄, DMF, 70 °C; followed by NaOH, EtOH: H₂O 1:1, 40 °C, 37-89%; (b) (2-(methoxycarbonyl)phenyl)boronic acid, CsF, Pd(dppf)•DCM, dioxane, H₂O, 60 °C, followed by NaOH, EtOH: H₂O 1:1, rt, 31% of **21c**; (c) **21a**, acetic anhydride, 90 °C, followed by LiOH, THF: H₂O 1:1, rt, 98% of **22a**; (d) *t*-butylnitrite, DMF, 65 °C, 91% of **22b** (from **21a**), 71% of **22c** (from **21d**).

A Suzuki-coupling reaction of the commercially available starting materials **23a** and **23b** with 4-methoxycarbonylphenyl boronic acid afforded intermediates **24a** and **24b** in 35% and 76% yield, respectively (Scheme 3). Hydrolysis of **24b** under mild conditions with lithium hydroxide gave the carboxylic acid functionalized allosteric moieties **25** in modest yield (27%). Intermediate **24a** underwent a second Suzuki-coupling reaction with (3-(trifluoromethyl)phenyl)boronic acid to afford **26** in 64% yield, followed by the hydrolysis of the ester group with sodium hydroxide in ethanol and water to give the carboxylic acid intermediate **27** in good yield (83%).

Scheme 3. Synthesis of the functionalized allosteric A₁AR pharmacophores **25 and **27**^a**

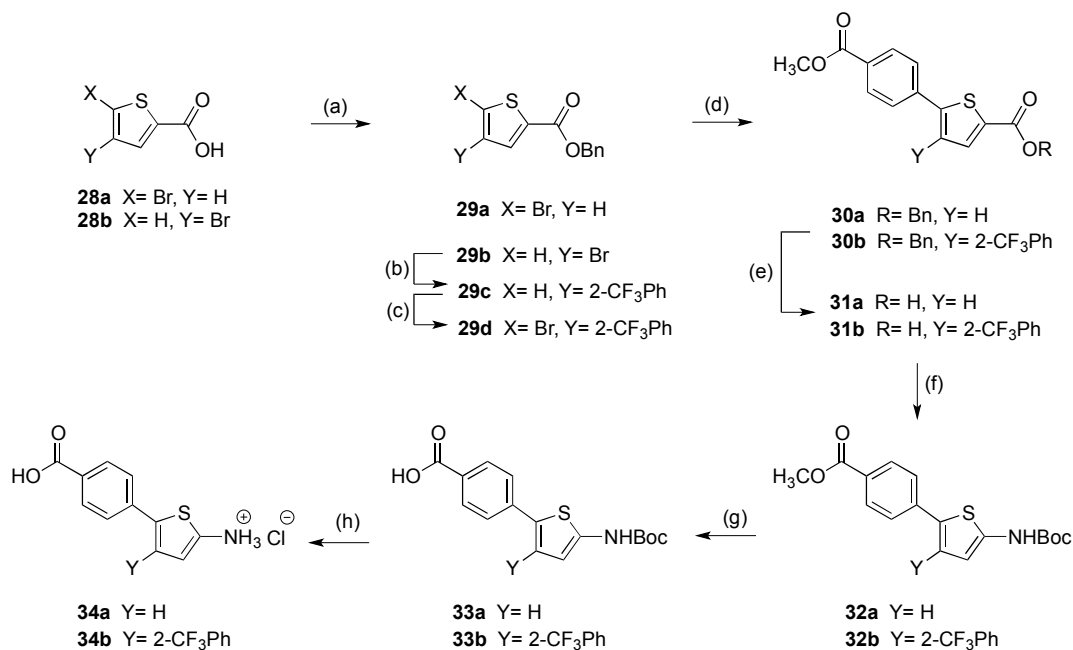


^aReagents and conditions: (a) (4-(methoxycarbonyl)phenyl)boronic acid, Pd(PPh₃)₂Cl₂, 2 M K₃PO₄, DMF, 80 °C, 35% of **24a**, 76% of **24b**; (b) LiOH, EtOH: H₂O 1:1, 27%; (c) (3-(trifluoromethyl)phenyl)boronic acid, Pd(PPh₃)₂Cl₂, 2 M K₃PO₄, DMF, 80 °C, 64%; (d) NaOH, EtOH: H₂O 3:1, rt, 83%.

The multistep synthesis of **34a** and **34b** (Scheme 4) started from the commercially available 5- or 4-bromothiophene-2-carboxylic acids **28a** and **28b**, respectively. First, the carboxylic acid functional group was protected with a benzyl group to give **29a** and **b** in quantitative yields. In the case of **29b**, a trifluoromethylphenyl substituent was introduced in the 4-position via a Suzuki-coupling reaction and the resulting product **29c** was brominated in position 5 with *N*-bromosuccinimide (NBS) to give **29d** in 66% yield. The bromine intermediates **29a** and **29d** were reacted with (4-(methoxycarbonyl)phenyl)boronic acid under Suzuki-coupling conditions to afford **30a** and **30b**, subsequent debenzylation via hydrogenation with Pd/C gave intermediates **31a** and **31b**, respectively. Next, the carboxylic acid group was converted to an acyl azide with diphenylphosphoryl azide (DPPA) in *tert*-butanol, followed by an *in situ* Curtius rearrangement to form the *tert*-butyloxycarbonyl (Boc) protected intermediates **32a** and **32b**. These key intermediates were then hydrolysed to the carboxylic acid analogues (**33a** and **33b**), followed by the final Boc-deprotection under acidic conditions to form the hydrochloride salts **34a** and **34b**.

Finally, the carboxylic acid functionalized allosteric moieties **21a–d**, **22a–c**, **25**, **27** and **34a–b** were linked to the orthosteric counterpart to form the final bitopic ligands **2–16**, which were fully characterized and assessed in our pharmacological assays.

Scheme 4. Synthesis of the functionalized allosteric A₁AR pharmacophores **34a–b^a**



^aReagents and conditions: (a) BnBr, TBAI, Cs₂CO₃, DMF, rt, 98%; (b) (3-(trifluoromethyl)phenyl)boronic acid, CsF, Pd(dppf)•DCM, dioxane, H₂O, 60 °C, 66%; (c) NBS, AcOH, 60 °C, 100%; (d) (4-(methoxycarbonyl)phenyl)boronic acid, CsF, Pd(dppf)•DCM, dioxane, H₂O, 60 °C, 76-84%; (e) H₂, Pd/C, EtOAc, DMF or *i*PrOH, 82-89%; (f) *tert*-BuOH, DPPA, Et₃N, rt, 69-71%; (g) 2 M NaOH, (dioxane), EtOH, H₂O, 85-98%; (h) 4 M HCl, dioxane, 87-100%.

Pharmacology. *cAMP accumulation assays.* The A₁AR preferentially couples to G_{i/o} proteins, leading to a decrease in adenylyl cyclase activity and subsequent cAMP accumulation. As such, the ability of NECA (a non-selective adenosine receptor agonist), **1** and the bitopic derivatives (**2–16**) to inhibit forskolin-stimulated cAMP accumulation was assessed in FlpIn-CHO cells stably expressing the human A₁AR (A₁AR-FlpIn-CHO). Data were fitted to a three-parameter Hill equation and a re-parameterization of the operational model of agonism. The Hill equation

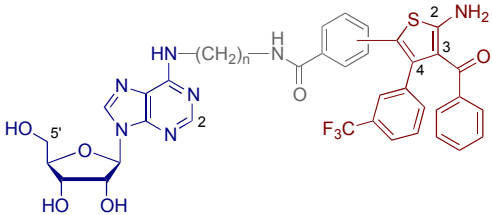
provided estimation of agonist potency (pEC_{50}) and maximal effect (E_{MAX}), whereas the operational model enabled quantification of the agonist transduction coefficient ($\text{Log}(\tau/K_A)$), a composite value of agonist affinity (K_A) and efficacy (τ).²⁵ The transduction coefficient is a useful parameter for comparative pharmacology, particularly for agonists that have different maximal effects (E_{MAX}), as incorporating both agonist efficacy and affinity enables a more global measure of agonist activity. Subsequent normalization of $\text{Log}(\tau/K_A)$ values to the reference agonist NECA generated $\Delta\text{Log}(\tau/K_A)$, a system independent measurement of agonist activity that was used for the quantification of bias and subtype selectivity.

Modification to the orthosteric pharmacophore (i.e. the introduction of a 2-amino, 2-chloro or 5'-*N*-ethylcarboxamide moieties in **2**, **3** and **4**, respectively) resulted in a significant reduction of $\text{Log}(\tau/K_A)$ relative to the parent compound **1** (Table 1). In contrast, linker modifications had differential effects. Decreasing the linker length by one methylene unit (**5**) had no significant effect, while incorporation of an additional methylene linker (**6**) resulted in a significant increase in the $\text{Log}(\tau/K_A)$. Varying the point of attachment of the thiophene to the linker from a *para* to an *ortho* substitution pattern (**8**) resulted in a significant decrease in the pEC_{50} and $\text{Log}(\tau/K_A)$. A number of modifications were also made to the allosteric pharmacophore. Neither acetylation or removal of the amino substituent on the thiophene ring (**9** and **10**, respectively) nor individual or dual removal of the benzoyl or trifluoromethylphenyl groups from the thiophene (**11**, **12** and **15**) had a significant effect on the pEC_{50} or $\text{Log}(\tau/K_A)$. However, the $\text{Log}(\tau/K_A)$ was significantly reduced upon removal of the amino group together with one or both of the other thiophene substituents (**13**, **14** and **16**). All derivatives had a similar E_{MAX} for cAMP inhibition, relative to the non-selective full agonist NECA (Table 1).

These structure-activity-relationships differ from what has been previously observed for 'stand-alone' A_1AR agonists and allosteric modulators. For example, the introduction of a 2-chloro group or 5'-*N*-ethylcarboxamide to an N^6 -substituted adenosine has been shown to increase potency at the A_1AR .^{26,27} Similarly, the removal of the 3-benzoyl moiety from a 2-amino-3-benzoylthiophene

1 PAM abolishes activity. These differences in SAR profiles suggest that presence of the linker
2
3 induces a different binding mode for the bitopic molecules relative to the stand-alone agonist and
4
5
6 allosteric modulator components.
7
8
9
10
11
12
13
14
15
16
17
18
19
20
21
22
23
24
25
26
27
28
29
30
31
32
33
34
35
36
37
38
39
40
41
42
43
44
45
46
47
48
49
50
51
52
53
54
55
56
57
58
59
60

Table 1. A₁AR Receptor Pharmacology: Inhibition of cAMP Accumulation and Stimulation of Intracellular Calcium Mobilization.



- Orthosteric Pharmacophore**
- 2 2-NH₂
 - 3 2-Cl
 - 4 5'-C(O)NH₂
- Linker Modifications**
- 5 n= 5
 - 6 n= 7
 - 7 *meta* thiophene
 - 8 *ortho* thiophene
- Allosteric Pharmacophore**
- 9 2-NHC(O)CH₃
 - 10 des 2-NH₂
 - 11 des 3-C(O)Ph
 - 12 des 4-PhCF₃
 - 13 des 2-NH₂ + des 3-C(O)Ph
 - 14 des 2-NH₂ + des 4-PhCF₃
 - 15 des 3-C(O)Ph + des 4-PhCF₃
 - 16 des 2-NH₂ + des 3-C(O)Ph + des 4-PhCF₃

Cpd	cAMP				Calcium			
	pEC ₅₀	E _{Max}	Log(τ/K _A)	n	pEC ₅₀	E _{Max}	Log(τ/K _A)	n
NECA	9.12 ± 0.08	101 ± 3	8.98 ± 0.09	10	9.36 ± 0.11	54 ± 2	9.31 ± 0.11	12
1	7.37 ± 0.07	112 ± 4	7.35 ± 0.07	3	6.91 ± 0.24	34 ± 5#	6.12 ± 0.34	6
2	5.87 ± 0.05****	115 ± 4	6.01 ± 0.04****	4	6.59 ± 0.38	34 ± 9	6.15 ± 0.43	3
3	6.65 ± 0.11**	106 ± 5	6.70 ± 0.03**	4	6.87 ± 0.26	20 ± 4###	6.32 ± 0.21	3
4	7.01 ± 0.16	112 ± 8	6.80 ± 0.09**	4	7.25 ± 0.40	16 ± 5####	6.33 ± 0.23	3
5	7.02 ± 0.08	114 ± 6	6.98 ± 0.08	3	7.13 ± 0.25	31 ± 4#	6.11 ± 0.42	3
6	7.64 ± 0.10	105 ± 5	7.85 ± 0.13*	3	6.70 ± 0.45	28 ± 8#	5.58 ± 0.71	3
7	6.98 ± 0.19	99 ± 9	6.97 ± 0.23	3	7.03 ± 0.06	48 ± 1	6.98 ± 0.05	3
8	5.89 ± 0.20****	104 ± 15	5.89 ± 0.15****	3	5.87 ± 0.05	43 ± 1	5.74 ± 0.05	3
9	6.86 ± 0.11	119 ± 9	6.97 ± 0.06	3	6.05 ± 0.71	20 ± 16###	5.02 ± 0.43	3
10	6.96 ± 0.08	114 ± 6	6.93 ± 0.11	3	6.25 ± 0.48	40 ± 17	5.74 ± 0.43	3
11	7.42 ± 0.13	110 ± 6	7.44 ± 0.10	3	6.96 ± 0.11	42 ± 2	6.86 ± 0.06	3
12	7.38 ± 0.11	101 ± 5	7.21 ± 0.04	3	7.53 ± 0.06	49 ± 1	7.43 ± 0.01*	3
13	6.77 ± 0.08*	106 ± 5	6.64 ± 0.15****	3	7.11 ± 0.06	49 ± 1	7.03 ± 0.05	3
14	6.86 ± 0.17	109 ± 9	6.86 ± 0.09*	3	7.06 ± 0.11	39 ± 2	6.91 ± 0.03	3
15	7.17 ± 0.17	100 ± 7	7.04 ± 0.15	3	7.46 ± 0.10	47 ± 2	7.40 ± 0.01*	3
16	6.63 ± 0.10**	117 ± 6	6.69 ± 0.09**	3	7.45 ± 0.08	49 ± 1	7.38 ± 0.06*	3

Data represents the mean ± SEM of 3 to 12 separate experiments conducted in duplicate or triplicate. * P<0.05, ** P<0.01, *** P<0.001, **** P<0.0001 derivative value (pEC₅₀ or Log(τ/K_A)) was significantly different (one-way analysis of variance, Dunnett's post-hoc) compared to the parent compound, 1, at the corresponding pathway. # P<0.05, ## P<0.01, ### P<0.001, significantly different (one-way analysis of variance, Dunnett's post-hoc) when compared to the NECA E_{MAX} at the corresponding pathway. Curves for parent compound, 1, were taken from Baltos *et al.*¹⁹

Biased agonism at the A_1AR . The influence of structural modifications on A_1AR biased agonism was also investigated. We have previously demonstrated that in A_1AR -FlpIn-CHO cells, compound **1** has significant bias away from calcium mobilization, relative to the reference pathway cAMP and the reference ligand, NECA.¹⁹ The current study has quantitatively evaluated the influence of various structural components of **1** on calcium mobilization (Table 1) and bias (Figure 2A). Bias was quantified by normalizing agonist $\text{Log}(\tau/K_A)$ values to the $\text{Log}(\tau/K_A)$ value of the reference agonist, NECA; subsequently, these values were normalized to the reference pathway, cAMP accumulation, to generate $\text{Log}(\text{Bias Factor})$ values.¹⁹

Modification to the orthosteric pharmacophore or linker had no significant effect on the pEC_{50} or $\text{Log}(\tau/K_A)$ value, relative to **1**, for A_1AR -mediated calcium mobilization (Table 1). In contrast, single deletion of the 4-(trifluoromethyl)phenyl, dual deletion of the 4-(trifluoromethyl)phenyl in conjunction with the benzoyl or triple deletion of all three substituents from the allosteric moiety resulted in a significant increase in the $\text{Log}(\tau/K_A)$ value for calcium mobilization (Table 1). These findings suggest the 4-(trifluoromethyl)phenyl substituent on the allosteric pharmacophore impedes A_1AR -mediated calcium mobilization.

Addition of a 2-amino group to the purine scaffold with the orthosteric pharmacophore (**2**) resulted in a significant loss of bias relative to **1**, such that this compound was non-biased (Figure 2A). The change in bias resulted from a decrease in the cAMP $\Delta\text{Log}(\tau/K_A)$ with little reduction in the calcium $\Delta\text{Log}(\tau/K_A)$ (Figure 2B). Interestingly, increasing the linker length by one additional carbon, as in compound **6**, resulted in approximately 10-fold increase in bias away from calcium mobilization, relative to compound **1**, however this effect did not reach significance (Figure 2A). The change in the compound **6** bias factor arises due to an increase in the cAMP $\Delta\text{Log}(\tau/K_A)$ but a decrease in the calcium $\Delta\text{Log}(\tau/K_A)$ (Figure 2B). We have previously shown that bitopic linker length exhibits a bell-shaped relationship with ligand affinity and potency.¹³ Accordingly, the effects of the linker length on bias may reflect an improvement or weakening in the engagement of

the allosteric or orthosteric pharmacophore with their corresponding binding pockets,²⁸⁻³⁰ thereby enhancing or reducing biased signaling, respectively. Changing the position of the thiophene scaffold from the *para* to the *meta*-position (7) significantly decreased the degree of bias, suggesting that the orientation of the allosteric pharmacophore is also important for biased signaling (Figure 2A).

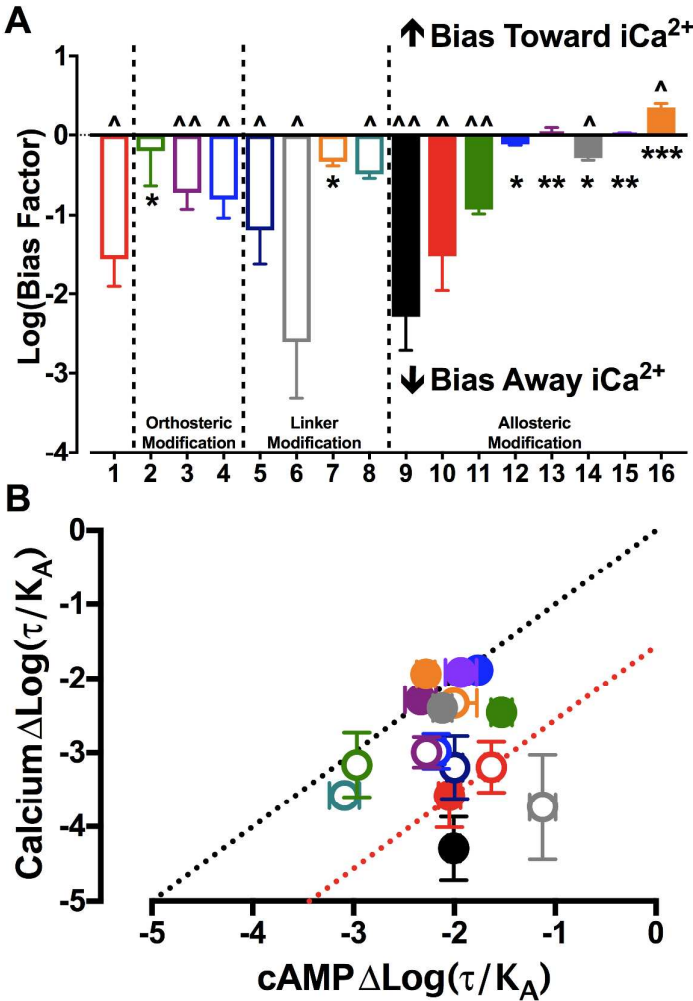


Figure 2. (A) Bias factors for **1** and derivatives at the A₁AR for the calcium mobilization pathway, relative to the reference ligand NECA and the reference pathway cAMP. Agonist Log(τ/K_A) values were normalized to the Log(τ/K_A) of the reference ligand, NECA, at each respective pathway to generate ΔLog(τ/K_A) values. These were then normalized to the cAMP pathway, to generate the Log(Bias Factor). *P<0.05, **P<0.01, One-way ANOVA Dunnett's post-hoc analysis when compared to the Log(Bias Factor) of **1**. ^P<0.05, ^^P<0.01, unpaired t-test comparing the calcium

$\Delta\text{Log}(\tau/K_A)$ and cAMP $\Delta\text{Log}(\tau/K_A)$. (B) Calcium $\Delta\text{Log}(\tau/K_A)$ and cAMP $\Delta\text{Log}(\tau/K_A)$ values are plotted relative to each other to visualize the relative contribution of each value to the calculated $\text{Log}(\text{Bias Factor})$. Values that fall upon the slope of unity (black dotted line) represent ligands with no bias between calcium mobilization and cAMP inhibition. Agonists that fall upon the slope of 1 (red dotted line) have a similar bias as that of **1**, as there is a similar magnitude of difference between the calcium $\Delta\text{Log}(\tau/K_A)$ and cAMP $\Delta\text{Log}(\tau/K_A)$ values. Data represent the mean \pm SEM from 3 to 12 independent experiments performed in duplicate or triplicate.

Acetylation or removal of the amino group on the allosteric thiophene pharmacophore (*c.f.* compound **9** and **10**, respectively) did not significantly influence the bias profile when compared to the parent compound; although **9** trended towards an increase in bias relative to **1** (Figure 2A). Similarly, the removal of the benzoyl group (compound **11**) had no significant effect on the bias profile observed (Figure 2A). However, removal of the 4-(trifluoromethyl)phenyl group (compound **12**) or two or more of the thiophene substituents (compounds **13–16**) significantly reduced the bias away from calcium mobilization, relative to compound **1** (Figure 2A). Interestingly, compound **16**, in which three of the thiophene substituents have been deleted, showed a reversal in the bias profile relative to compound **1**, such that it demonstrated significant bias toward calcium mobilization (Figure 2A). These findings highlight the importance of the allosteric moiety substituents, particularly the 4-(trifluoromethyl)phenyl on the thiophene scaffold in retaining a biased signaling profile away from calcium mobilization.

Investigating the impact of structural modifications to adenosine receptor subtype selectivity.

To investigate the influence of structural modifications on adenosine receptor subtype selectivity, additional studies were performed using FlpIn-CHO cells stably expressing the human $A_{2A}\text{AR}$ ($A_{2A}\text{AR}$ -FlpIn-CHO), human $A_{2B}\text{AR}$ ($A_{2B}\text{AR}$ -FlpIn-CHO) or human $A_3\text{AR}$ ($A_3\text{AR}$ -FlpIn-CHO). At the $A_{2A}\text{AR}$, all ligands except compound **8**, stimulated a detectable level of cAMP accumulation, with no significant difference in the maximal effect (Table 2). A significant increase in the $A_{2A}\text{AR}$ pEC_{50} and $\text{Log}(\tau/K_A)$, relative to **1**, was observed upon modification of the 2- and 5'-positions of

orthosteric pharmacophore (compounds **3** and **4**, respectively), relocation of the thiophene ring from the *para* to the *meta*-position (compound **7**), and deletion of the trifluoromethylphenyl substituent of the thiophene ring (compound **12**) (Table 2). At the A_{2B}AR, the structural modifications had no significant effect on the pEC₅₀, E_{MAX} or Log(τ /K_A), with the exception of **16**, which had a significantly increased Log(τ /K_A) (Table 2). At the A₃AR, compounds **2** and **3** had no significant activity at any concentration employed (up to 10 μ M). Additionally, the activity of **5** and **10** was too low to be adequately defined. An increase in the Log(τ /K_A), relative to **1**, was observed for **6**, **7** and **8**, which have modified linkers, and **15**, which has two substituents deleted from the thiophene (Table 2). Relative to NECA, the parent compound **1**, and the derivatives **6**, **9**, **11** and **13** were partial agonists at the A₃AR (Table 2).

The influence of structural modifications on the selectivity index, relative to the A₁AR, was established at each adenosine receptor subtype for modulation of cAMP accumulation. Agonist Log(τ /K_A) values were normalized to the corresponding NECA Log(τ /K_A), thereby forming Δ Log(τ /K_A). This value represents a system independent measurement of agonist activity at each adenosine receptor subtype, which was subsequently normalized relative to the A₁AR to establish the selectivity index and thus quantify subtype selectivity. The selectivity index reflects a ratio of the Δ Log(τ /K_A) determined for each agonist at each subtype, relative to the Δ Log(τ /K_A) determined for the A₁AR. The selectivity index is expressed on a log scale, whereby a selectivity index equal to zero reflects no subtype selectivity between the A₁AR and corresponding subtype, relative to NECA. In contrast, values greater than or less than zero reflect an increase or decrease in subtype selectivity relative to the A₁AR, respectively.

The selectivity index, normalized to the non-selective agonist NECA, demonstrated that **1** had greatest selectivity for the A_{2B}AR, followed by the A₁AR, A₃AR then A_{2A}AR. Modification of the orthosteric pharmacophore (compounds **2-4**) resulted in a significant increase in the A_{2A}AR selectivity index, with each of these compounds demonstrating preference for the A_{2A}AR over the

A₁AR (Figure 3). Similarly, **12-14** and **16**, which incorporated thiophene substituent deletions, resulted in an increase in the A_{2A}AR selectivity index, such that these compounds were non-selective for the A₁AR and A_{2A}AR (Figure 3). Compound **6**, in which the linker length is increased by one carbon, exhibits significantly greater A₁AR selectivity relative to the A_{2A}AR. Compound **7** (*meta*-substituted) had modest A_{2A}AR selectivity, whereas **8** (*ortho*-substituted) showed no appreciable A_{2A}AR activity, and therefore exhibited A₁AR selectivity (Figure 3). As observed previously,³¹ **1** is a relatively high potency A_{2B}AR agonist, with greater selectivity relative to NECA, for the A_{2B}AR over the A₁AR (Figure 3). Whilst most derivatives maintained a similar degree of selectivity to that of **1**, some modifications had significantly greater preference for the A_{2B}AR. These included derivatives with modification to the 2-position of the purine group (**2** and **3**) and complete truncation of substituents on the thiophene ring (**16**), each of which had an approximate 200-fold greater A_{2B}AR selectivity index over the other adenosine receptor subtypes. The increase in A_{2B}AR subtype selectivity relative to the A₁AR, for compounds **2** and **3** resulted predominantly from a decrease in the A₁AR Log(τ/K_A), whereas the increased A_{2B}AR subtype selectivity relative to the A₁AR, for **16** is due to combined increase and decrease in the A_{2B}AR and A₁AR Log(τ/K_A), respectively. A significant increase in the A₃AR selectivity index was observed when the allosteric pharmacophore was shifted from the *para* to the *meta* or *ortho*-position (compounds **7** and **8**, respectively). Indeed, **7** and **8** had approximately 10-fold and 100-fold greater relative selectivity for the A₃AR than the A₁AR, respectively (Figure 3). These findings suggest modification of the linker region may enable the generation of a bivalent ligand with A₃AR selectivity.

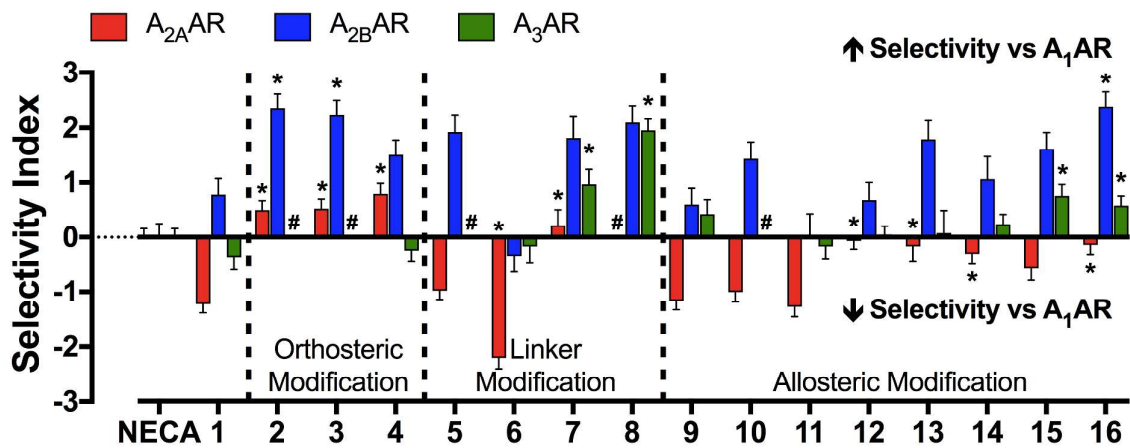
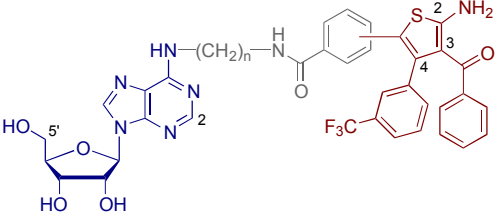


Figure 3. The subtype selectivity of **1** and derivatives at the four adenosine receptor subtypes, relative to the non-selective agonist NECA. The subtype selectivity index was utilized to attain a system-independent measurement of agonist subtype selectivity. Values are logarithmic and, when equal to zero, indicate no subtype selectivity relative to the A₁AR, whereas values greater than or less than zero reflect an increase or decrease in the subtype selectivity relative to the A₁AR, respectively. *P<0.05, one-way ANOVA Dunnett's post-hoc analysis when compared to the selectivity index of **1** at the corresponding adenosine receptor subtype. #Subtype selectivity index could not be determined due to minimal activity. Data represent the mean \pm SEM from 3 to 10 independent experiments performed in duplicate or triplicate.

Table 2. Subtype Selectivity of VCP746 and Derivatives in Human AR Expressing FlpIn-CHO Cells at the cAMP Pathway.



Orthosteric Pharmacophore

2 2-NH₂

3 2-Cl

4 5'-C(O)NHet

Linker Modifications

5 n= 5

6 n= 7

7 *meta* thiophene

8 *ortho* thiophene

Allosteric Pharmacophore

9 2-NHC(O)CH₃

10 des 2-NH₂

11 des 3-C(O)Ph

12 des 4-PhCF₃

13 des 2-NH₂ + des 3-C(O)Ph

14 des 2-NH₂ + des 4-PhCF₃

15 des 3-C(O)Ph + des 4-PhCF₃

16 des 2-NH₂ + des 3-C(O)Ph + des 4-PhCF₃

Cpd		A ₁ -FlpInCHO	A _{2A} -FlpInCHO	A _{2B} -FlpInCHO	A ₃ -FlpInCHO
NECA	pEC ₅₀	9.12 ± 0.08	8.48 ± 0.10	7.80 ± 0.18	7.85 ± 0.09
	E _{Max}	101 ± 3	105 ± 3	40 ± 3	97 ± 3
	Log(τ/K _A)	8.98 ± 0.09	8.53 ± 0.08	7.65 ± 0.16	7.94 ± 0.08
	n	10	6	7	6
1	pEC ₅₀	7.37 ± 0.07	5.64 ± 0.11	7.02 ± 0.30	6.10 ± 0.17
	E _{Max}	112 ± 4	109 ± 9	37 ± 5	49 ± 6 ^{###}
	Log(τ/K _A)	7.35 ± 0.07	5.67 ± 0.09	6.80 ± 0.22	5.94 ± 0.17
	n	3	3	4	4
2	pEC ₅₀	5.87 ± 0.05****	6.12 ± 0.16	7.01 ± 0.22	ND
	E _{Max}	115 ± 4	111 ± 11	43 ± 4	ND
	Log(τ/K _A)	6.01 ± 0.04****	6.07 ± 0.12	7.03 ± 0.18	ND
	n	4	3	4	3
3	pEC ₅₀	6.65 ± 0.11**	6.84 ± 0.10***	7.73 ± 0.23	ND
	E _{Max}	106 ± 5	110 ± 5	39 ± 3	ND
	Log(τ/K _A)	6.70 ± 0.03**	6.78 ± 0.13****	7.60 ± 0.19	ND
	n	4	3	4	3
4	pEC ₅₀	7.01 ± 0.16	7.25 ± 0.12****	7.12 ± 0.24	5.85 ± 0.17
	E _{Max}	112 ± 8	114 ± 6	38 ± 4	75 ± 8
	Log(τ/K _A)	6.80 ± 0.09**	7.15 ± 0.12****	6.97 ± 0.18	5.51 ± 0.13
	n	4	3	4	4
5	pEC ₅₀	7.02 ± 0.08	5.44 ± 0.27	7.20 ± 0.22	<6
	E _{Max}	114 ± 6	131 ± 34	52 ± 5	ND
	Log(τ/K _A)	6.98 ± 0.08	5.56 ± 0.09	7.58 ± 0.23	<6
	n	3	3	4	3

6	pEC ₅₀	7.64 ± 0.10	5.31 ± 0.13	6.33 ± 0.26	6.48 ± 0.29
	E _{Max}	105 ± 5	97 ± 13	38 ± 5	56 ± 13 [#]
	Log(τ/K _A)	7.85 ± 0.13*	5.20 ± 0.10*	6.18 ± 0.17	6.64 ± 0.23*
	n	3	3	5	3
7	pEC ₅₀	6.98 ± 0.19	6.83 ± 0.21***	7.45 ± 0.30	6.91 ± 0.19
	E _{Max}	99 ± 9	83 ± 10	43 ± 5	80 ± 6
	Log(τ/K _A)	6.97 ± 0.23	6.75 ± 0.13****	7.45 ± 0.26	6.90 ± 0.09**
	n	3	3	3	3
8	pEC ₅₀	5.89 ± 0.20****	ND	6.54 ± 0.22	6.55 ± 0.21
	E _{Max}	104 ± 15	ND	46 ± 5	103 ± 11
	Log(τ/K _A)	5.89 ± 0.15****	ND	6.66 ± 0.19	6.80 ± 0.09**
	n	3	3	4	3
9	pEC ₅₀	6.86 ± 0.11	5.63 ± 0.37	6.21 ± 0.31	6.35 ± 0.47
	E _{Max}	119 ± 9	91 ± 31	44 ± 8	60 ± 25 [#]
	Log(τ/K _A)	6.97 ± 0.06	5.35 ± 0.09	6.25 ± 0.23	6.36 ± 0.23
	n	3	3	4	3
10	pEC ₅₀	6.96 ± 0.08	5.54 ± 0.14	6.83 ± 0.24	<6
	E _{Max}	114 ± 6	101 ± 13	49 ± 5	ND
	Log(τ/K _A)	6.93 ± 0.11	5.48 ± 0.09	7.03 ± 0.22	<6
	n	3	3	4	3
11	pEC ₅₀	7.42 ± 0.13	5.57 ± 0.11	6.35 ± 0.40	6.55 ± 0.17
	E _{Max}	110 ± 6	127 ± 12	28 ± 6	58 ± 6 [#]
	Log(τ/K _A)	7.44 ± 0.10	5.72 ± 0.09	6.15 ± 0.34	6.23 ± 0.16
	n	3	3	4	3
12	pEC ₅₀	7.38 ± 0.11	6.45 ± 0.08*	6.65 ± 0.35	6.35 ± 0.21
	E _{Max}	101 ± 5	110 ± 5	40 ± 6	85 ± 11
	Log(τ/K _A)	7.21 ± 0.04	6.69 ± 0.09****	6.56 ± 0.27	6.22 ± 0.09
	n	3	3	3	3
13	pEC ₅₀	6.77 ± 0.08*	6.19 ± 0.22	7.04 ± 0.29	6.46 ± 0.27
	E _{Max}	106 ± 5	61 ± 9	44 ± 5	26 ± 5 ^{####}
	Log(τ/K _A)	6.64 ± 0.15***	6.03 ± 0.19	7.10 ± 0.25	5.68 ± 0.37
	n	3	3	3	3

14	pEC₅₀	6.86 ± 0.17	6.36 ± 0.15	6.80 ± 0.40	6.39 ± 0.15
	E_{Max}	109 ± 9	86 ± 7	27 ± 5	74 ± 7
	Log(τ/K_A)	6.86 ± 0.09*	6.10 ± 0.09	6.59 ± 0.36	6.06 ± 0.10
	n	3	3	3	3
15	pEC₅₀	7.17 ± 0.17	5.97 ± 0.12	7.22 ± 0.20	7.19 ± 0.15**
	E_{Max}	100 ± 7	106 ± 8	45 ± 4	72 ± 5
	Log(τ/K_A)	7.04 ± 0.15	6.02 ± 0.09	7.33 ± 0.19	6.76 ± 0.09*
	n	3	3	4	3
16	pEC₅₀	6.63 ± 0.10**	5.88 ± 0.10	7.75 ± 0.21	6.08 ± 0.10
	E_{Max}	117 ± 6	105 ± 9	42 ± 3	107 ± 7
	Log(τ/K_A)	6.69 ± 0.09**	6.11 ± 0.10	7.74 ± 0.19*	6.24 ± 0.09
	n	3	3	4	3

Data represents the mean ± SEM of 3 to 10 separate experiments conducted in duplicate or triplicate (A₁-FlpInCHO data from Table 1 included for clarity). * P<0.05, ** P<0.01, *** P<0.001, **** P<0.0001 derivative value was significantly different (one-way analysis of variance, Dunnett's post-hoc) compared to the corresponding parameter for **1** at the corresponding adenosine receptor subtype. # P<0.05, ## P<0.01, ### P<0.001, significantly different (one-way analysis of variance, Dunnett's post-hoc) when compared to the NECA E_{MAX} at the corresponding adenosine receptor subtype.

Molecular Modeling. Molecular modelling employed an active A₁AR homology model based on the recent crystal structure of A_{2A}AR co-bound with agonist NECA and an engineered G protein.³² Incorporated within the active A₁AR homology model were several extracellular loop (ECL) features present in the A₁AR inactive crystal structure (PDB ID: 5UEN)³⁰ such as the disulfide bonds, the ECL2 alpha helices and the ECL1/ECL2 short beta sheet. Adenosine docked within the transmembrane (TM) bundle, where the adenine ring was stabilized by a hydrogen bond with the conserved residue, N254^{6,55} and π -stacking interaction with ECL2, F171^{ECL2} (Figure 4). The orientation of adenine moiety within this active A₁AR homology model was similar to that reported for the agonist-bound A_{2A}AR crystal structures (PDB ID: 2YDO; PDB ID: 5G53).^{32,33} Docking of compound **1** within the active A₁AR homology model, used a template docking method where the adenosine moiety was constrained to the docking pose determined for adenosine alone. The linker region of compound **1** was stabilized by a hydrogen bond between the amide group and E170^{ECL2} and hydrophobic interaction with E172^{ECL2} (Figure 4). The allosteric moiety of compound **1** was predicted to bind to an extracellular cage bordered by the top of TM5, TM6, the alpha-helical region of ECL2 and ECL3. Specifically, the hydrophilic surface of this moiety was oriented toward ECL3, with the 2-amino and the 3-keto groups of the thiophene ring anchored by hydrogen bond interactions with S262^{ECL3}, whereas the 4-(trifluoromethyl)phenyl group of the thiophene ring formed hydrophobic interaction with E172^{ECL2}, K173^{ECL2}, T257^{6,58} and H264^{ECL3} (Figure 4).

Deletion of the 4-(trifluoromethyl)phenyl group resulted in a loss of biased agonism suggesting that predicted hydrophobic interactions within the extracellular vestibule are key for A₁AR biased agonism (Figure 2, Figure 4). This finding is in accordance with previous studies demonstrating that the addition of the 4-(trifluoromethyl)phenyl moiety can enhance the A₁AR allosteric modulator activity of 2-amino-3-benzoylthiophenes (2A3BTs). Interestingly, certain modifications of the 2-amino-3-benzoylthiophene (2A3BT) unit that are known to have a significant effect on allosteric activity³⁴ (e.g. acetylation or removal of the 2-amino group in compounds **9** and **10**) have

afforded bitopic ligands with a biased profile similar to **1** (Figure 2). This may well be a result of the 2A3BT moiety of these bitopic compounds adopting a different binding pose relative to stand-alone 2A3BT allosteric modulators. Indeed, the predicted binding pose for the allosteric pharmacophore of compound **1**, is different to the predicted binding pose of the corresponding stand-alone 2A3BT.²⁹ It is unsurprising that the attachment of a very large linker and adenosine moiety to the relatively low affinity allosteric modulator might alter, to some extent, the binding mode of the allosteric moiety within compound **1**.

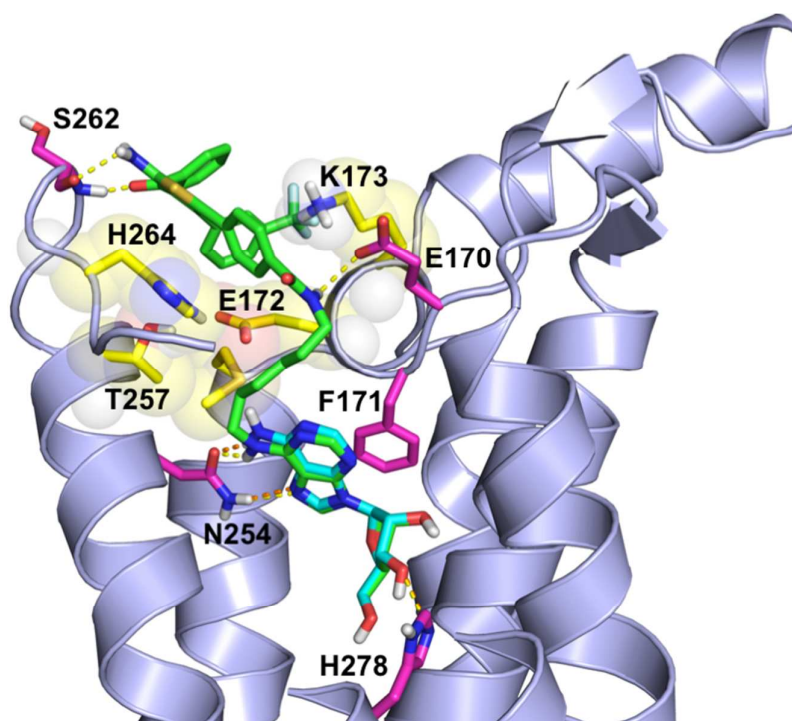


Figure 4. Docking of compound **1** (green) and adenosine (cyan) into an active A_1AR homology model based on an active $A_{2A}AR$ crystal structure (PDB ID: 5G53). Residues contributing to hydrogen bonds and π -stacking interactions are highlighted in magenta, whereas residues that form key hydrophobic interactions are highlighted in yellow.

■ CONCLUSIONS

This study has provided the first insight into the molecular determinants and SAR of the novel bitopic ligands at the A₁AR. Overall, our findings suggest that the allosteric pharmacophore, particularly the 4-(trifluoromethyl)phenyl substituent, has an important role in governing bitopic ligand bias at the A₁AR. Importantly, single deletion of the 4-(trifluoromethyl)phenyl substituent (**12**) abolished the bias whereas removal of all three substituents of the thiophene scaffold (**16**) resulted in a reversal in the bias, such that at the A₁AR, compound **16** was significantly biased towards calcium mobilization. Furthermore, these data highlight that extending the alkyl linker length by one carbon ($n = 7$, compound **6**) trended to increase both the bias and A₁AR selectivity, relative to **1**. As such, compounds **6**, **12** and **16** represent novel tools to interrogated the mechanistic basis of A₁AR bias in cardiac (patho)physiology. Our docking studies suggest that interactions of the allosteric moiety and linker region within the extracellular vestibule may underlie the initial trigger of the biased agonist profile of compound **1**. Interestingly, the predicted binding pose for tethered allosteric moiety within the *N*⁶-substituted adenosine derivative **1** is different to the corresponding untethered allosteric modulator.²⁹ Collectively, these findings will inform future structure-based drug design efforts for the development of clinically relevant adenosine receptor biased agonists.

■ EXPERIMENTAL SECTION

Chemistry. Chemicals and solvents were purchased from standard suppliers and used without further purification. Davisil[®] silica gel (40-63 μm) for flash column chromatography was supplied by Grace Davison Discovery Sciences (Victoria, Australia) and deuterated solvents were purchased from Cambridge Isotope Laboratories, Inc. (USA, distributed by Novachem PTY. Ltd, Victoria, Australia).

Unless otherwise stated, reactions were carried out at ambient temperature. Reactions were monitored by thin layer chromatography on commercially available pre-coated aluminium-backed plates (Merck Kieselgel 60 F₂₅₄). Visualisation was by examination under UV light (254 and 366 nm). All organic extracts collected after aqueous work-up procedures were dried over anhydrous MgSO_4 or Na_2SO_4 before gravity filtering and evaporation to dryness. Organic solvents were evaporated *in vacuo* at $\leq 40^\circ\text{C}$ (water bath temperature). Purification using preparative layer chromatography (PLC) was carried out on Analtech preparative TLC plates (200 mm x 200 mm x 2 mm).

^1H NMR and ^{13}C NMR spectra were recorded on a Bruker Avance Nanobay III 400MHz Ultrashield Plus spectrometer at 400.13 MHz and 100.62 MHz, respectively. Chemical shifts (δ) are recorded in parts per million (ppm) with reference to the chemical shift of the deuterated solvent. Coupling constants (J) and carbon-fluorine coupling constants (J_{CF}) are recorded in Hz and the significant multiplicities described by singlet (s), doublet (d), triplet (t), quadruplet (q), broad (br), multiplet (m), doublet of doublets (dd), doublet of triplets (dt).

Preparative HPLC was performed using an Agilent 1260 infinity coupled with a binary preparative pump and Agilent 1260 FC-PS fraction collector, using Agilent OpenLAB CDS software (Rev C.01.04), and an Altima 5 μM C8 22 x 250 mm column. The following buffers were

used; buffer A: H₂O; buffer B: MeCN, with sample being run at a gradient of 30% buffer B to 100% buffer B over 10 min, at a flow rate of 20 mL/min.

LC-MS were run to verify reaction outcome and purity using an Agilent 1200 Series HPLC coupled to an Agilent 6100 Series Single Quad MS system or an Agilent 1260 Series HPLC coupled to an Agilent 6120 Series Single Quad MS system. The following buffers were used; buffer A: 0.1% formic acid in H₂O; buffer B: 0.1% formic acid in MeCN. The following gradient was used with a Poroshell 120 EC-C18 50 x 3.0 mm 2.7 micron column, and a flow rate of 0.5 mL/min and total run time of 5 min; 0–1 min 95% buffer A and 5% buffer B, from 1–2.5 min up to 0% buffer A and 100% buffer B, held at this composition until 3.8 min, 3.8–4 min 95% buffer A and 5% buffer B, held until 5 min at this composition. All screening compounds were of > 95% purity. Mass spectra were acquired in positive and negative ion mode with a scan range of 100–1000 *m/z*. UV detection was carried out at 214 and 254 nm. All retention times (*t_R*) are quoted in min. HRMS analyses were carried out on an Agilent 6224 TOF LC/MS Mass Spectrometer coupled to an Agilent 1290 Infinity (Agilent, Palo Alto, CA). All data were acquired and reference mass corrected via a dual-spray electrospray ionisation (ESI) source. Acquisition was performed using the Agilent Mass Hunter Data Acquisition software version B.05.00 Build 5.0.5042.2 and analysis was performed using Mass Hunter Qualitative Analysis version B.05.00 Build 5.0.519.13.

General amide coupling procedure used for the synthesis of final compounds 1-16. Respective acid (1.0 eq) and respective amine (1.0 eq) were dissolved in anhydrous DMF (3 mL/100 mg), to this solution was added BOP (1.5 eq) followed by Et₃N (5.0 eq). The reaction was stirred at rt until full conversion was observed, followed by an individual work-up and purification procedure.

4-(5-Amino-4-benzoyl-3-(3-(trifluoromethyl)phenyl)thiophen-2-yl)-N-(6-((2-amino-9-((2R,3R,4S,5R)-3,4-dihydroxy-5-(hydroxymethyl)tetrahydrofuran-2-yl)-9H-purin-6-yl)amino)hexyl)benzamide (2). EtOAc (100 mL) was added before being washed with H₂O (2 ×

50 mL) and brine (1 × 50 mL). The organic layer was dried with Na₂SO₄, filtered and the solvent removed under reduced pressure. Purification by column chromatography (eluent DCM: MeOH 100:0 → 90:10) gave the titled product as a yellow solid (76 mg, 43%). ¹H NMR (*d*₆-DMSO) δ 8.39 (t, *J* = 5.6 Hz, 1H), 8.27 (s, 2H), 7.95 (s, 1H), 7.72–7.65 (m, 2H), 7.39–7.26 (m, 2H), 7.23–7.12 (m, 6H), 7.08–6.98 (m, 4H), 5.85–5.74 (m, 3H), 5.58–5.48 (m, 1H), 5.40 (d, *J* = 6.3 Hz, 1H), 5.15 (d, *J* = 4.5 Hz, 1H), 4.56 (dd, *J* = 11.4, 6.2 Hz, 1H), 4.18–4.10 (m, 1H), 3.96 (q, *J* = 3.4 Hz, 1H), 3.74–3.64 (m, 1H), 3.63–3.54 (m, 1H), 3.48–3.41 (m, 2H), 3.31–3.20 (m, 2H), 1.67–1.48 (m, 4H), 1.43–1.30 (m, 4H); ¹³C NMR (*d*₆-DMSO) δ 192.2, 166.4, 165.8, 160.4, 155.5, 140.6, 137.3, 136.5, 136.3, 135.2, 134.7, 133.1, 130.3, 129.2, 128.9, 128.8 (q, *J* = 31.9 Hz), 128.4, 127.7, 127.5, 127.4 (q, *J* = 3.7 Hz), 124.2 (q, *J* = 272 Hz), 123.6 (q, *J* = 3.9 Hz), 119.2, 115.9, 87.5, 86.0, 73.7, 71.2, 62.2, 39.9, 39.6, 29.6 (2C), 26.8, 26.7; LCMS *R*_f (min) = 3.19. MS *m/z* 831.3 (M + H); HRMS – C₄₁H₄₂F₃N₈O₆S [M+H]⁺ calcd 831.2900, found 831.2927.

4-(5-Amino-4-benzoyl-3-(3-(trifluoromethyl)phenyl)thiophen-2-yl)-N-(6-((2-chloro-9-((2*R*,3*R*,4*S*,5*R*)-3,4-dihydroxy-5-(hydroxymethyl)tetrahydrofuran-2-yl)-9*H*-purin-6-yl)amino)hexyl)benzamide (3). EtOAc (100 mL) was added before being washed with H₂O (2 × 50 mL) and brine (1 × 50 mL). The organic layer was dried with Na₂SO₄, filtered and the solvent removed under reduced pressure. The crude product was purified twice by column chromatography (eluent DCM: MeOH 100:0 → 90:10) to give the titled product as a yellow solid (8 mg, 6%). ¹H NMR (*d*₄-MeOD) δ 8.22 (s, 1H), 7.64–7.58 (m, 2H), 7.20–7.13 (m, 3H), 7.12–7.03 (m, 6H), 7.01–6.94 (m, 2H), 5.92 (d, *J* = 6.2 Hz, 1H), 4.71–4.66 (m, 1H), 4.33 (dd, *J* = 5.1, 2.9 Hz, 1H), 4.17 (q, *J* = 2.7 Hz, 1H), 3.91 (dd, *J* = 12.5, 2.6 Hz, 1H), 3.77 (dd, *J* = 12.5, 2.9 Hz, 1H), 3.56 (br t, *J* = 6.6 Hz, 2H), 3.38–3.34 (m, 2H), 1.75–1.59 (m, 4H), 1.54–1.39 (m, 4H); LCMS *R*_f (min) = 3.41. MS *m/z* 849.7 (M + H); HRMS – C₄₁H₄₀ClF₃N₇O₆S [M+H]⁺ calcd 850.2401, found 850.2399.

(2*S*,3*S*,4*R*,5*R*)-5-(6-((6-Aminohexyl)amino)-9*H*-purin-9-yl)-N-ethyl-3,4-dihydroxytetrahydrofuran-2-carboxamide (4). The reaction mixture was evaporated to dryness

and the residue was taken up in EtOAc (200 mL) before being washed with H₂O (3 × 100 mL). The organic layer was dried with Na₂SO₄, filtered and evaporated to dryness. Purification by column chromatography (eluent DCM: MeOH 9:1) gave the titled compound as a yellow oil (24 mg, 15%). ¹H NMR (*d*₃-MeOD) δ 8.27 (s, 1H), 8.24 (s, 1H), 7.62–7.59 (m, 2H), 7.18–7.14 (m, 3H), 7.11–7.04 (m, 6H), 6.99–6.95 (m, 2H), 6.02 (d, *J* = 7.72 Hz, 1H), 4.76 (dd, *J* = 4.8 Hz, 1H), 4.48 (d, *J* = 1.52 Hz, 1H), 4.33 (dd, *J* = 1.28 Hz, 1H), 3.59 (br s, 2H), 3.40–3.32 (m, 4H), 1.72 (quin, *J* = 7.08 Hz, 2H), 1.62 (quin, *J* = 7.36 Hz, 2H), 1.48–1.42 (m, 4H), 1.21 (t, *J* = 7.28 Hz, 3H); ¹³C NMR (*d*₃-MeOD) δ 193.5, 170.7, 168.0, 167.6, 140.4, 137.2, 137.0, 135.2, 134.1, 132.6, 129.8, 129.5, 129.35 (q, *J* = 30.3 Hz), 128.8, 128.7, 128.3, 127.9 (2C), 127.3 (q, *J* = 4.1 Hz), 127.2, 126.9, 123.8 (q, *J* = 271.5 Hz), 123.0 (q, *J* = 3.8 Hz), 89.1, 85.1, 73.6, 72.0, 119.8, 115.7, 53.4, 39.5, 33.7, 29.0 (2C), 26.4, 26.2, 13.8; LCMS *R*_f (min) = 3.41. MS *m/z* 857.3 (M + H); HRMS – C₄₃H₄₄F₃N₈O₆S [M+H]⁺ calcd 857.3057, found 857.3080.

4-(5-Amino-4-benzoyl-3-(3-(trifluoromethyl)phenyl)thiophen-2-yl)-N-(5-((9-((2*R*,3*R*,4*S*,5*R*)-3,4-dihydroxy-5-(hydroxymethyl)tetrahydrofuran-2-yl)-9*H*-purin-6-yl)amino)pentyl)benzamide (5). The product mixture was added dropwise via syringe to 100 mL ice/water, a bright yellow precipitate formed, the suspension was stirred for 30 min and was allowed to settle in the fridge (-5 °C). The solution was filtered and the solid washed with cold H₂O, before being dried under vacuum for 12 h. This gave 196 mg crude solid which was dry loaded onto a silica column (eluent CHCl₃: MeOH: NH₄OH_{aq} 90:10:1). Concentration of the appropriate fractions gave a residue, which was triturated with cold Et₂O. Filtration and washing with cold Et₂O, before drying under vacuum gave a yellow solid (156 mg, 90%). ¹H NMR (*d*₆-DMSO) δ 8.35–8.31 (m, 2H), 8.23–8.17 (m, 3H), 7.90–7.84 (m, 1H), 7.65–7.60 (m, 2H), 7.27–7.22 (m, 1H), 7.15–7.08 (m, 6H), 7.00–6.94 (m, 4H), 5.87 (d, *J* = 6.0 Hz, 1H), 5.45–5.42 (m, 2H), 5.17 (d, *J* = 4.4 Hz, 1H), 4.61 (q, *J* = 6.0 Hz, 1H), 4.16–4.12 (m, 1H), 3.96 (q, *J* = 3.2 Hz, 1H), 1.60 (quin, *J* = 7.2 Hz, 2H), 1.51 (quin, *J* = 7.2 Hz, 2H), 1.36–1.28 (m, 2H); ¹³C NMR (*d*₆-DMSO) δ

191.7, 165.9, 165.3, 154.6, 152.3, 148.2, 140.2, 139.6, 136.8, 136.1, 134.8, 134.2, 132.6, 129.8, 128.7, 128.5, 128.3 (q, $J = 31.3$ Hz), 127.9, 127.2 (2C), 126.9 (q, $J = 3.9$ Hz), 123.8 (q, $J = 270.0$ Hz), 123.2 (q, $J = 4.2$ Hz), 119.9, 118.8, 115.4, 88.0, 85.9, 73.4, 70.7, 61.7, 39.2, 28.8, 23.9; HRMS – $C_{40}H_{39}F_3N_7O_6S$ $[M+H]^+$ calcd 802.2629, found 802.2626.

4-(5-Amino-4-benzoyl-3-(3-(trifluoromethyl)phenyl)thiophen-2-yl)-N-(7-((9-((2R,3R,4S,5R)-3,4-dihydroxy-5-(hydroxymethyl)tetrahydrofuran-2-yl)-9H-purin-6-yl)amino)heptyl)benzamide (6). The product mixture was added dropwise via syringe to 100 mL ice/water, a bright yellow precipitate formed, the suspension was stirred for 30 min and was allowed to settle in the fridge (-5 °C). The solution was filtered and the solid washed with cold H_2O , before being dried under vacuum for 12 h. This gave 195 mg crude solid which was dry loaded onto a silica column (eluent $CHCl_3$: MeOH: NH_4OH_{aq} 90:10:1). Concentration of the appropriate fractions gave a residue, which was triturated with cold Et_2O . Filtration and washing with cold Et_2O , before drying under vacuum gave a yellow solid (127 mg, 72%). 1H NMR (d_6 -DMSO) δ 8.34–8.30 (m, 2H), 8.22–8.19 (m, 3H), 7.91–7.86 (m, 1H), 7.62 (dt, $J = 6.8, 2.0$ Hz, 2H), 7.26–7.23 (m, 1H), 7.14–7.07 (m, 6H), 7.00–6.94 (m, 4H), 5.87 (d, $J = 6.2$ Hz, 1H), 5.44–5.42 (m, 2H), 5.17 (d, $J = 4.4$ Hz, 1H), 4.61 (q, $J = 6.2$ Hz, 1H), 4.16–4.12 (m, 1H), 3.96 (q, $J = 3.2$ Hz, 1H), 1.56 (quin, $J = 6.4$ Hz, 2H), 1.45 (quin, $J = 6.4$ Hz, 2H), 1.34–1.22 (m, 6H); ^{13}C NMR (d_6 -DMSO) δ 191.7, 165.9, 165.3, 154.7, 152.3, 148.2, 140.2, 139.6, 136.8, 136.1, 134.8, 134.2, 132.6, 129.9, 128.7, 128.4, 128.4 (q, $J = 31.4$ Hz), 127.9, 127.2 (2C), 127.0 (q, $J = 4.2$ Hz), 123.8 (q, $J = 270.9$ Hz), 123.2 (q, $J = 3.6$ Hz), 119.8, 118.8, 115.4, 88.0, 85.9, 79.2, 73.5, 70.7, 61.7, 39.2, 29.0, 28.6, 26.5, 26.4; HRMS – $C_{42}H_{43}F_3N_7O_6S$ $[M+H]^+$ calcd 830.2942, found 830.2937.

3-(5-Amino-4-benzoyl-3-(3-(trifluoromethyl)phenyl)thiophen-2-yl)-N-(6-((9-((2R,3R,4S,5R)-3,4-dihydroxy-5-(hydroxymethyl)tetrahydrofuran-2-yl)-9H-purin-6-yl)amino)hexyl)benzamide (7). The mixture was slowly diluted with H_2O (50 mL) and extracted with $EtOAc$ (3×50 mL). The combined organic layers were washed with H_2O (2×50 mL), brine

(50 mL) and then dried with MgSO_4 , filtered and concentrated to a yellow/orange foam (479 mg). The crude was dissolved in a minimum of 95:5:1, CHCl_3 : MeOH: $\text{NH}_4\text{OH}_{\text{aq}}$ and chromatographed on silica gel (eluent CHCl_3 : MeOH: $\text{NH}_4\text{OH}_{\text{aq}}$ 95:5:1 \rightarrow 90:10:1). The appropriate fractions were concentrated to a resin that was sonicated in EtOH and filtered providing an amorphous solid (54 mg, 9%). ^1H NMR (d_6 -DMSO) δ 8.40–8.29 (m, 2H), 8.24–8.14 (m, 3H), 7.95–7.83 (m, 1H), 7.63–7.54 (m, 2H), 7.23–7.16 (m, 2H), 7.16–7.04 (m, 6H), 7.00–6.91 (m, 3H), 5.88 (d, J = 6.2 Hz, 1H), 5.47–5.40 (m, 2H), 5.18 (d, J = 4.5 Hz, 1H), 4.61 (dd, J = 11.4, 5.9 Hz, 1H), 4.14 (dd, J = 7.6, 4.6 Hz, 1H), 3.96 (dd, J = 6.1, 3.0 Hz, 1H), 3.67 (dt, J = 11.9, 3.9 Hz, 1H), 3.60–3.38 (m, 3H), 3.18 (dd, J = 12.7, 6.6 Hz, 2H), 1.65–1.23 (m, 8H); ^{13}C NMR (d_6 -DMSO) δ 192.1, 166.2, 165.9, 155.1, 152.9, 148.7, 140.6, 140.1, 137.2, 135.4, 134.9, 134.6, 133.8, 131.9, 130.3, 129.0, 128.7, 128.5, 128.4, 128.3 (q, J = 31.2 Hz), 127.6, 127.5, 127.4, 126.1, 123.5 (q, J = 272.2 Hz), 120.2, 119.5, 115.6, 88.4, 86.4, 73.9, 71.2, 62.2, 39.0, 29.5, 29.5, 26.7, 26.7; LCMS R_f (min) = 5.86. MS m/z 816.2 ($\text{M} + \text{H}$); HRMS – $\text{C}_{41}\text{H}_{41}\text{F}_3\text{N}_7\text{O}_6\text{S}$ [$\text{M} + \text{H}$] $^+$ calcd 816.2786, found 816.2790.

2-(5-Amino-4-benzoyl-3-(3-(trifluoromethyl)phenyl)thiophen-2-yl)-N-(6-((9-((2*R*,3*R*,4*S*,5*R*)-3,4-dihydroxy-5-(hydroxymethyl)tetrahydrofuran-2-yl)-9*H*-purin-6-yl)amino)hexyl)benzamide (8). The mixture was slowly diluted with H_2O (20 mL) and extracted with EtOAc (3×50 mL). The combined organic layers were washed with H_2O (2×50 mL), brine (50 mL) and then dried with MgSO_4 , filtered and concentrated to a yellow gum. The crude was chromatographed on silica (eluent CHCl_3 : MeOH: $\text{NH}_4\text{OH}_{\text{aq}}$ 95:5:1 \rightarrow 90:10:1). The appropriate fractions were concentrated to a resin that was dissolved in EtOH and precipitated with H_2O (125 mg, 78%). ^1H NMR (d_6 -DMSO) δ 8.34 (s, 1H), 8.20 (s, 1H), 8.11 (s, 3H), 7.86 (s, 1H), 7.36–7.24 (m, 2H), 7.20–7.04 (m, 7H), 7.00–6.86 (m, 4H), 5.89 (d, J = 6.1 Hz, 1H), 5.52–5.38 (m, 2H), 5.20 (d, J = 4.5 Hz, 1H), 4.62 (dd, J = 11.1, 5.7 Hz, 1H), 4.22–4.08 (m, 1H), 4.03–3.91 (m, 1H), 3.73–3.64 (m, 1H), 3.61–3.52 (m, 1H), 3.46 (s, 2H), 3.18–3.03 (m, 2H), 1.66–1.40 (m, 4H), 1.40–1.25 (m, 4H); ^{13}C NMR (d_6 -DMSO) δ 191.0, 168.0, 166.2, 154.7, 152.4, 148.2, 140.1, 139.7, 139.2,

137.0, 134.6, 133.9, 132.3, 131.3, 129.9, 129.0, 128.1, 128.1 (q, $J = 10.2$ Hz), 128.0, 127.7, 127.4, 127.1, 126.8 (q, $J = 3.7$ Hz), 123.9 (q, $J = 272.4$ Hz), 122.4 (q, $J = 3.7$ Hz), 119.8, 119.0, 88.0, 86.0, 73.5, 70.7, 61.8, 39.0, 29.0, 29.0 26.3, 26.3; LCMS R_f (min) = 5.79. MS m/z 816.2 (M + H); HRMS – $C_{41}H_{41}F_3N_7O_6S$ [M+H]⁺ calcd 816.2786, found 816.2795.

4-(5-Acetamido-4-benzoyl-3-(3-(trifluoromethyl)phenyl)thiophen-2-yl)-N-(6-((9-((2R,3R,4S,5R)-3,4-dihydroxy-5-(hydroxymethyl)tetrahydrofuran-2-yl)-9H-purin-6-yl)amino)hexyl)benzamide (9). The product mixture was added dropwise via syringe to 100 mL ice/water, a bright yellow precipitate formed, the suspension was stirred for 30 min and was allowed to settle in the fridge (-5 °C). The solution was filtered and the solid washed with cold H₂O, before being dried under vacuum for 12 h. This gave 145 mg crude solid which was dry loaded onto a silica column (eluent CHCl₃: MeOH: NH₄OH_{aq} 90:10:1). Concentration of the appropriate fractions gave a residue, which was triturated with cold Et₂O. Filtration and washing with cold Et₂O, before drying under vacuum gave a yellow solid (91 mg, 51%). ¹H NMR (*d*₆-DMSO) δ 10.99 (s, 1H), 8.39 (t, $J = 5.6$ Hz, 1H), 8.32 (s, 1H), 8.20–8.16 (m, 1H), 7.91–7.82 (m, 1H), 7.72–7.68 (m, 2H), 7.52–7.48 (m, 2H), 7.42–7.36 (m, 2H), 7.29–7.17 (m, 7H), 5.87 (d, $J = 6.0$ Hz, 1H), 5.44–5.41 (m, 2H), 5.17 (d, $J = 4.8$ Hz, 1H), 4.61 (q, $J = 6.0$ Hz, 1H), 4.15–4.12 (m, 1H), 3.95 (q, $J = 3.2$ Hz, 1H), 3.67 (dt, $J = 12.0, 4.0$ Hz, 1H), 3.58–3.41 (m, 3H), 3.20 (q, $J = 6.4$ Hz, 2H), 2.14 (s, 3H), 1.62–1.54 (m, 2H), 1.52–1.44 (m, 2H), 1.36–1.27 (m, 4H); ¹³C NMR (*d*₆-DMSO) δ 192.7, 168.4, 165.3, 154.6, 152.3, 148.2, 142.1, 139.6, 137.6, 135.9, 135.3, 134.0, 133.4, 132.9, 132.7, 129.4, 129.1, 128.7, 128.6 (q, $J = 31.8$ Hz), 128.0, 127.4, 126.6 (q, $J = 3.5$ Hz), 124.5, 123.7 (q, $J = 270.8$ Hz), 123.7 (q, $J = 3.8$ Hz), 119.7, 87.9, 85.9, 73.4, 70.7, 61.7, 39.2, 29.0, 26.3, 26.2, 22.6; HRMS – $C_{43}H_{43}F_3N_7O_7S$ [M+H]⁺ calcd 858.2891, found 858.2888.

4-(4-Benzoyl-3-(3-(trifluoromethyl)phenyl)thiophen-2-yl)-N-(6-((9-((2R,3R,4S,5R)-3,4-dihydroxy-5-(hydroxymethyl)tetrahydrofuran-2-yl)-9H-purin-6-yl)amino)hexyl)benzamide (10). The product mixture was added dropwise via syringe to 100 mL ice/water, a bright yellow

precipitate formed, the suspension was stirred for 30 mins and was allowed to settle in the fridge (-5°C). The solution was filtered and the solid washed with cold H₂O, before being dried under vacuum for 12 h. This gave 196 mg crude solid which was dry loaded onto a silica column (eluent CHCl₃: MeOH: NH₄OH_{aq} 90:10:1). Concentration of the appropriate fractions gave a residue which was triturated with cold Et₂O. Filtration and washing with cold Et₂O, before drying under vacuum gave a yellow solid (78 mg, 46%). ¹H NMR (*d*₆-DMSO) δ 8.44 (t, *J* = 5.6 Hz, 1H), 8.33 (s, 1H), 8.19 (s, 1H), 7.90–7.85 (m, 1H), 7.78–7.73 (m, 1H), 7.65–7.36 (m, 7H), 7.27–7.25 (m, 2H), 5.87 (d, *J* = 6.0 Hz, 1H), 5.47–5.43 (m, 2H), 5.19 (d, *J* = 4.8 Hz, 1H), 4.61 (q, *J* = 6.0 Hz, 1H), 4.16–4.13 (m, 1H), 3.96 (q, *J* = 3.2 Hz, 1H), 3.67 (dt, *J* = 12.0, 4.0 Hz, 1H), 3.58–3.52 (m, 1H), 3.50–3.43 (m, 2H), 3.21 (q, *J* = 6.0 Hz, 2H), 1.58 (quin, *J* = 6.4 Hz, 2H), 1.49 (quin, *J* = 6.8 Hz), 1.38–1.29 (m, 4H); ¹³C NMR (*d*₆-DMSO) δ 190.8, 165.3, 154.7, 152.3, 141.1, 140.6, 139.6, 137.4, 136.9, 136.0, 135.0, 134.1, 134.0, 133.2, 132.8, 129.5, 129.2, 128.9, 128.8 (q, *J* = 31.1 Hz), 128.5, 127.5, 126.5 (q, *J* = 3.7 Hz), 123.9 (q, *J* = 270.5 Hz), 123.9 (q, *J* = 3.5 Hz), 119.7, 118.9, 88.0, 85.9, 73.5, 70.7, 61.7, 39.2, 29.0, 26.3, 26.2; HRMS – C₄₁H₄₀F₃N₆O₆S [M+H]⁺ calcd 801.2677, found 801.2692.

4-(5-Amino-3-(3-(trifluoromethyl)phenyl)thiophen-2-yl)-N-(6-((9-((2*R*,3*R*,4*S*,5*R*)-3,4-dihydroxy-5-(hydroxymethyl)tetrahydrofuran-2-yl)-9*H*-purin-6-yl)amino)hexyl)benzamide (11). The mixture was slowly diluted with H₂O (50 mL) and extracted with EtOAc (3 × 50 mL). The combined organic layers were washed with H₂O (2 × 50 mL), brine (50 mL) and then dried with MgSO₄, filtered and concentrated (630 mg). The crude was chromatographed on silica gel (eluent CHCl₃: MeOH: NH₄OH_{aq} 95:5:1 → 90:10:1). The appropriate fractions were concentrated to a resin that was sonicated in EtOAc providing an amber coloured amorphous solid (78 mg, 16%). ¹H NMR (*d*₆-DMSO) δ 8.39–8.29 (m, 2H), 8.25–8.12 (m, 1H), 7.95–7.81 (m, 1H), 7.67 (d, *J* = 8.4 Hz, 2H), 7.64–7.60 (m, 1H), 7.58–7.47 (m, 3H), 7.11 (d, *J* = 8.4 Hz, 2H), 6.04 (s, 1H), 6.00 (s, 2H), 5.88 (d, *J* = 6.2 Hz, 1H), 5.52–5.42 (m, 2H), 5.20 (d, *J* = 4.5 Hz, 1H), 4.62 (dd, *J* = 11.3, 5.9 Hz,

1H), 4.15 (dd, $J = 7.6, 4.6$ Hz, 1H), 3.97 (dd, $J = 6.4, 3.3$ Hz, 1H), 3.68 (dt, $J = 12.0, 3.9$ Hz, 1H), 3.60–3.52 (m, 1H), 3.52–3.43 (m, 2H), 3.21 (dd, $J = 12.7, 6.5$ Hz, 2H), 1.68–1.54 (m, 2H), 1.54–1.42 (m, 2H), 1.40–1.25 (m, 4H); ^{13}C NMR (d_6 -DMSO) δ 165.6, 154.7, 152.5, 148.2, 139.7, 138.0, 137.0, 136.3, 132.7, 131.9, 129.8, 129.4 (q, $J = 31.6$ Hz), 127.5, 127.5, 125.0 (q, $J = 3.8$ Hz), 124.1 (q, $J = 272.3$ Hz), 123.7 (q, $J = 3.7$ Hz), 119.8, 119.4, 107.2, 88.1, 86.0, 73.5, 70.8, 61.8, 39.2, 29.2, 29.1, 26.4, 26.3; LCMS R_f (min) = 5.58. MS m/z 712.2 (M + H); HRMS – $\text{C}_{34}\text{H}_{37}\text{F}_3\text{N}_7\text{O}_5\text{S}$ [M+H] $^+$ calcd 712.2523, found 712.2547.

4-(5-Amino-4-benzoylthiophen-2-yl)-N-(6-((9-((2R,3R,4S,5R)-3,4-dihydroxy-5-(hydroxymethyl)tetrahydrofuran-2-yl)-9H-purin-6-yl)amino)hexyl)benzamide (12). The mixture was slowly diluted with H_2O (≈ 30 mL) and a yellow precipitate formed. The solid was filtered on a Buchner funnel/flask and washed with copious amounts of H_2O and finally Et_2O and then suck dried. The precipitate was dissolved in a minimum of DMF (2 mL) and precipitated with CHCl_3 : MeOH: $\text{NH}_4\text{OH}_{\text{aq}}$ 90:10:1 (2 mL) and stirred for several hours. The precipitate was collected and washed with EtOH and finally Et_2O providing the yellow precipitate as an amorphous solid (47 mg, 41%). ^1H NMR (d_6 -DMSO) δ 8.66 (s, 2H), 8.40 (t, $J = 5.5$ Hz, 1H), 8.33 (s, 1H), 8.19 (s, 1H), 7.95–7.83 (m, 1H), 7.79 (d, $J = 8.5$ Hz, 2H), 7.70–7.64 (m, 2H), 7.60–7.45 (m, 5H), 7.25 (s, 1H), 5.88 (d, $J = 6.2$ Hz, 1H), 5.48–5.39 (m, 2H), 5.18 (d, $J = 4.6$ Hz, 1H), 4.61 (dd, $J = 11.3, 6.0$ Hz, 1H), 4.14 (dd, $J = 7.7, 4.6$ Hz, 1H), 3.96 (dd, $J = 6.2, 3.1$ Hz, 1H), 3.67 (dt, $J = 11.9, 4.0$ Hz, 1H), 3.60–3.41 (m, 3H), 3.23 (dd, $J = 12.7, 6.5$ Hz, 2H), 1.64–1.47 (m, 4H), 1.41–1.27 (m, 4H); ^{13}C NMR (d_6 -DMSO) δ 189.4, 167.3, 165.5, 154.7, 152.4, 148.2, 140.6, 139.6, 136.1, 132.1, 130.7, 2×128.4 , 2×127.9 , 2×123.8 , 120.8, 119.8, 114.1, 88.0, 85.9, 73.5, 70.7, 61.7, 39.1, 29.2, 29.1, 26.3, 26.2; LCMS R_f (min) = 5.32. MS m/z 672.2 (M + H); HRMS – $\text{C}_{34}\text{H}_{38}\text{N}_7\text{O}_6\text{S}$ [M+H] $^+$ calcd 672.2599, found 672.2620.

N-(6-((9-((2R,3R,4S,5R)-3,4-dihydroxy-5-(hydroxymethyl)tetrahydrofuran-2-yl)-9H-purin-6-yl)amino)hexyl)-4-(3-(3-(trifluoromethyl)phenyl)thiophen-2-yl)benzamide (13). The

mixture was slowly diluted with H₂O (30 mL) and extracted with EtOAc (3 × 50 mL). The combined organic layers were washed with H₂O (4 × 30 mL), brine (30 mL) and then dried with MgSO₄, filtered and concentrated to an opaque amorphous solid (641 mg). The crude was concentrated from EtOH (3 × 30 mL) and then sonicated in Et₂O (100 mL) to provide a powder. The powder was filtered and washed with Et₂O and suck dried providing a white amorphous solid (331 mg, 53%). ¹H NMR (*d*₆-DMSO) δ 8.46 (t, *J* = 5.5 Hz, 1H), 8.35 (s, 1H), 8.21 (s, 1H), 7.98–7.84 (m, 1H), 7.80 (d, *J* = 8.4 Hz, 2H), 7.73 (d, *J* = 5.2 Hz, 1H), 7.70–7.44 (m, 4H), 7.35 (d, *J* = 5.2 Hz, 1H), 7.32 (d, *J* = 8.4 Hz, 2H), 5.91 (d, *J* = 6.2 Hz, 1H), 5.54–5.42 (m, 2H), 5.21 (d, *J* = 4.6 Hz, 1H), 4.65 (dd, *J* = 11.3, 6.0 Hz, 1H), 4.18 (dd, *J* = 7.6, 4.7 Hz, 1H), 4.04–3.96 (m, 1H), 3.70 (dt, *J* = 11.9, 3.9 Hz, 1H), 3.63–3.40 (m, 3H), 3.25 (dd, *J* = 12.8, 6.6 Hz, 2H), 1.69–1.45 (m, 4H), 1.42–1.23 (m, 4H); ¹³C NMR (*d*₆-DMSO) δ 165.5, 154.7, 152.4, 148.2, 139.7, 136.8, 136.7, 135.9, 133.9, 132.9, 130.4, 129.7, 129.4 (q, *J* = 31.7 Hz), 128.8, 128.1, 127.7, 126.5, 125.2 (q, *J* = 3.6 Hz), 124.0 (q, *J* = 272.4 Hz), 123.8 (q, *J* = 3.7 Hz), 119.8, 88.1, 86.0, 73.6, 70.8, 64.9, 61.8, 39.3, 29.1, 29.1, 26.3, 26.2; LCMS *R*_f (min) = 6.21. MS *m/z* 697.2 (M + H); HRMS – C₃₄H₃₆F₃N₆O₅S [M+H]⁺ calcd 697.2415, found 697.2425.

4-(4-Benzoylthiophen-2-yl)-N-(6-((9-((2*R*,3*R*,4*S*,5*R*)-3,4-dihydroxy-5-(hydroxymethyl)tetrahydrofuran-2-yl)-9*H*-purin-6-yl)amino)hexyl)benzamide (14). The mixture was slowly diluted with H₂O (≈ 30 mL) and a brown/red precipitate formed. The precipitate was filtered on a Buchner funnel/flask and washed with copious amounts of H₂O and then suck dried (410 mg). The crude was chromatographed on silica gel (eluent DCM 100% → DCM: MeOH: NH₄OH_{aq} 95:5:0.1). The appropriate fractions were concentrated to a resin that was sonicated in a minimum of EtOH providing an amorphous straw coloured solid (150 mg, 35%). ¹H NMR (*d*₆-DMSO) δ 8.52 (t, *J* = 5.6 Hz, 1H), 8.36–8.31 (m, 1H), 8.26 (d, *J* = 1.4 Hz, 1H), 8.24–8.15 (m, 1H), 7.99 (d, *J* = 1.4 Hz, 1H), 7.97–7.93 (m, 1H), 7.91 (d, *J* = 8.5 Hz, 2H), 7.87–7.82 (m, 3H), 7.72–7.67 (m, 1H), 7.63–7.54 (m, 2H), 5.87 (d, *J* = 6.2 Hz, 1H), 5.48–5.39 (m, 2H), 5.18 (d, *J*

= 4.6 Hz, 1H), 4.61 (dd, J = 11.3, 6.0 Hz, 1H), 4.14 (dd, J = 7.7, 4.7 Hz, 1H), 3.96 (dd, J = 6.4, 3.3 Hz, 1H), 3.67 (dt, J = 12.0, 3.9 Hz, 1H), 3.58–3.51 (m, 1H), 3.51–3.43 (m, 2H), 3.26 (dd, J = 12.8, 6.6 Hz, 2H), 1.66–1.48 (m, 4H), 1.42–1.28 (m, 4H); ^{13}C NMR (d_6 -DMSO) δ 189.1, 165.5, 154.7, 152.5, 148.2, 143.5, 141.4, 139.7, 137.7, 135.4, 135.1, 134.2, 132.7, 129.2, 128.7, 128.2, 125.5, 124.9, 119.8, 88.0, 86.0, 73.5, 70.8, 61.8, 39.3, 29.2, 29.1, 26.4, 26.3; LCMS R_f (min) = 5.51. MS m/z 657.3 (M + H); HRMS – $\text{C}_{34}\text{H}_{37}\text{N}_6\text{O}_6\text{S}$ [M+H] $^+$ calcd 657.2490, found 657.2502.

4-(5-Aminothiophen-2-yl)-N-(6-((9-((2R,3R,4S,5R)-3,4-dihydroxy-5-(hydroxymethyl)tetrahydrofuran-2-yl)-9H-purin-6-yl)amino)hexyl)benzamide (15). The mixture was slowly diluted with H_2O (\approx 20 mL) and a brown precipitate formed. The precipitate was filtered on a Buchner funnel/flask and washed with copious amounts of H_2O and then suck dried (190 mg). The crude was chromatographed on silica gel (eluent DCM: MeOH: $\text{NH}_4\text{OH}_{\text{aq}}$ 100:0:0 \rightarrow 95:5:0.1). The appropriate fractions were concentrated providing an amorphous yellow/brown coloured solid (37 mg, 24%). ^1H NMR (d_6 -DMSO) δ 8.41–8.27 (m, 2H), 8.26–8.14 (m, 1H), 7.97–7.83 (m, 1H), 7.75 (d, J = 8.0 Hz, 2H), 7.42 (d, J = 7.9 Hz, 2H), 7.15 (d, J = 3.6 Hz, 1H), 6.04–5.92 (m, 2H), 5.93–5.83 (m, 2H), 5.53–5.40 (m, 2H), 5.25–5.14 (m, 1H), 4.62 (dd, J = 10.8, 5.5 Hz, 1H), 4.22–4.10 (m, 1H), 4.02–3.92 (m, 1H), 3.72–3.64 (m, 1H), 3.60–3.52 (m, 1H), 3.52–3.43 (m, 2H), 3.28–3.16 (m, 2H), 1.68–1.44 (m, 4H), 1.42–1.26 (m, 4H); ^{13}C NMR (d_6 -DMSO) δ 165.7, 155.9, 154.7, 152.5, 148.2, 139.7, 137.6, 130.7, 127.9, 124.9, 123.8, 122.7, 119.8, 105.0, 88.0, 86.0, 73.5, 70.8, 61.8, 39.2, 29.3, 29.1, 26.4, 26.3; LCMS R_f (min) = 4.87. MS m/z 568.3 (M + H); HRMS – $\text{C}_{27}\text{H}_{34}\text{N}_7\text{O}_5\text{S}$ [M+H] $^+$ calcd 568.2337, found 568.2357.

N-(6-((9-((2R,3R,4S,5R)-3,4-dihydroxy-5-(hydroxymethyl)tetrahydrofuran-2-yl)-9H-purin-6-yl)amino)hexyl)-4-(thiophen-2-yl)benzamide (16). The mixture was slowly diluted with H_2O (\approx 20 mL) and a white precipitate formed. The precipitate was filtered on a Buchner funnel/flask and washed with copious amounts of H_2O and then suck dried. The crude was dissolved in a minimum of CHCl_3 : MeOH: $\text{NH}_4\text{OH}_{\text{aq}}$ 95:5:1 and chromatographed on silica gel

(eluent DCM: MeOH: $\text{NH}_4\text{OH}_{\text{aq}}$ 95:5:1 \rightarrow 90:10:1). The appropriate fractions were concentrated to a resin that was sonicated in a minimum of EtOH providing an amorphous solid (62 mg, 35%). ^1H NMR (d_6 -DMSO) δ 8.47 (t, J = 5.5 Hz, 1H), 8.34 (s, 1H), 8.20 (s, 1H), 7.97–7.89 (m, 1H), 7.88 (d, J = 8.5 Hz, 2H), 7.73 (d, J = 8.5 Hz, 2H), 7.67–7.57 (m, 2H), 7.17 (dd, J = 5.1, 3.6 Hz, 1H), 5.88 (d, J = 6.2 Hz, 1H), 5.49–5.40 (m, 2H), 5.19 (d, J = 4.6 Hz, 1H), 4.62 (dd, J = 11.3, 6.1 Hz, 1H), 4.15 (dd, J = 7.7, 4.7 Hz, 1H), 3.97 (q, J = 3.3 Hz, 1H), 3.68 (dt, J = 12.0, 4.0 Hz, 1H), 3.59–3.52 (m, 1H), 3.52–3.39 (m, 2H), 3.25 (dd, J = 12.9, 6.6 Hz, 2H), 1.67–1.47 (m, 4H), 1.42–1.28 (m, 4H); ^{13}C NMR (d_6 -DMSO) δ 165.5, 154.7, 152.4, 148.2, 142.4, 139.7, 136.1, 133.4, 128.7, 128.1, 126.7, 125.0, 124.8, 119.8, 88.0, 86.0, 73.5, 70.7, 61.7, 39.2, 29.2, 29.1, 26.4, 26.2; LCMS R_f (min) = 5.24. MS m/z 553.3 (M + H); HRMS – $\text{C}_{27}\text{H}_{33}\text{N}_6\text{O}_5\text{S}$ [M+H] $^+$ calcd 553.2228, found 553.2240.

General synthesis of intermediates 19a-e. 6-Chloropurine version of orthosteric pharmacophore (**17a-c**) (1.0 eq), diaminoalkane (5.0 eq) and triethylamine (1.0 eq) were refluxed in ethanol (100 mL/ 2.5 g of the starting material) for 3 h under N_2 . Upon cooling to rt, a white solid precipitated was formed. The suspension was filtered, washed with cold ethanol and dried under high vacuum to afford the title product as a white powder.

(2*R*,3*R*,4*S*,5*R*)-2-(6-((5-aminopentyl)amino)-9*H*-purin-9-yl)-5-(hydroxymethyl)tetrahydrofuran-3,4-diol (19a). White powder (4.41 g, 90%). ^1H NMR (d_3 -MeOD) δ 8.24 (br s, 1H), 8.21 (br s, 1H), 5.95 (d, J = 6.4 Hz, 1H), 4.74 (t, J = 6.0 Hz, 1H), 4.32 (dd, J = 4.4, 2.0 Hz, 1H), 4.17–4.18 (m, 1H), 3.89 (dd, J = 12.4, 2.0 Hz, 1H), 3.74 (dd, J = 12.4, 2.4 Hz, 1H), 3.60 (br s, 2H), 2.67 (t, J = 6.8 Hz, 2H), 1.72 (quin, J = 6.8 Hz, 2H), δ 1.44–1.57 (m, 4H).

(2*R*,3*R*,4*S*,5*R*)-2-(6-((6-Aminohexyl)amino)-9*H*-purin-9-yl)-5-(hydroxymethyl)tetrahydrofuran-3,4-diol (19b). White powder (6.04 g, 90%). ^1H NMR (d_6 -DMSO) δ 8.34 (s, 1H), 8.21 (s, 1H), 7.90 (br s, 1H), 5.88 (d, J = 6.2 Hz, 1H), 5.46 (br s, 1H), 5.23 (br s, 1H), 4.62 (dd, J = 5.5, 5.5 Hz, 1H), 4.15 (dd, J = 4.8, 3.0 Hz, 1H), 4.00–3.94 (m, 1H), 3.68

(dd, $J = 12.1, 3.6$ Hz, 1H), 3.55 (dd, $J = 12.1, 3.5$ Hz, 1H), 3.50 – 3.42 (m, 2H), 3.33 (br s, 3H), 2.50–2.46 (m, 2H), 1.65–1.53 (m, 2H), 1.38–1.24 (m, 6H).

(2*R*,3*R*,4*S*,5*R*)-2-(6-((7-aminoheptyl)amino)-9*H*-purin-9-yl)-5-(hydroxymethyl)tetrahydrofuran-3,4-diol (19c). White powder (6.04 g, 92%). ^1H NMR (d_3 -MeOD) δ 8.24 (br s, 1H), 8.21 (br s, 1H), 5.95 (d, $J = 6.4$ Hz, 1H), 4.74 (dd, $J = 6.4, 5.2$ Hz, 1H), 4.32 (dd, $J = 5.2, 2.8$ Hz, 1H), 4.16–4.18 (m, 1H), 3.89 (dd, $J = 12.8, 2.4$ Hz, 1H), 3.74 (dd, $J = 12.4, 2.8$ Hz, 1H), 3.53–3.64 (m, 2H), 2.61 (t, $J = 7.2$ Hz, 2H), 1.70 (quin, $J = 7.2$ Hz, 2H), 1.35–1.50 (m, 8H).

(2*R*,3*R*,4*S*,5*R*)-2-(2-Amino-6-((6-aminohexyl)amino)-9*H*-purin-9-yl)-5-(hydroxymethyl)tetrahydrofuran-3,4-diol (19d). White powder (344 mg, 54%). ^1H NMR (d_6 -DMSO) δ 7.96 (s, 1H), 7.35 (br s, 1H), 5.90–5.70 (m, 3H), 4.60–4.53 (m, 1H), 4.18–4.12 (m, 1H), 3.99–3.93 (m, 1H), 3.70 (dd, $J = 12.0, 3.3$ Hz, 1H), 3.59 (dd, $J = 12.0, 3.2$ Hz, 1H), 3.54–3.00 (m, 5H), 2.50–2.46 (m, 2H), 1.66–1.56 (m, 2H), 1.42–1.28 (m, 8H).

(2*R*,3*R*,4*S*,5*R*)-2-(6-((6-aminohexyl)amino)-2-chloro-9*H*-purin-9-yl)-5-(hydroxymethyl)tetrahydrofuran-3,4-diol (19e). After the completion of the reaction the EtOH was evaporated under reduced pressure. The residue was taken up in DCM and left in the fridge overnight. The DCM layer was decanted and the titled product was obtained as the remaining light yellowish oil (66 mg, 18%). ^1H NMR (d_6 -DMSO) δ 8.38 (s, 1H), 7.28 (br s, 1H), 6.62 (br s, 1H), 5.82 (d, $J = 5.9$ Hz, 1H), 5.76 (s, 1H), 4.56–4.47 (m, 1H), 4.15–4.08 (m, 1H), 4.00–3.90 (m, 1H), 3.65 (dd, $J = 12.0, 3.3$ Hz, 1H), 3.37 (dd, $J = 12.0, 3.2$ Hz, 1H), 3.35–3.45 (m, 2H), 2.95–2.85 (m, 1H), 2.63–2.59 (m, 2H), 1.59 (s, 2H), 1.46–1.21 (m, 8H).

(2*S*,3*S*,4*R*,5*R*)-5-(6-((6-Aminoethyl)amino)-9*H*-purin-9-yl)-*N*-ethyl-3,4-dihydroxytetrahydrofuran-2-carboxamide (19f). 1,6-Diaminohexane (24.0 mg, 206 μmol , 1.0 eq) was dissolved in triethylamine (28.8 μL , 206 μmol , 1.0 eq) and EtOH (1 mL). To this, a

solution of (2*S*,3*S*,4*R*,5*R*)-*N*-Ethyl-3,4-dihydroxy-5-(6-oxo-1,6-dihydro-9*H*-purin-9-yl)tetrahydrofuran-2-carboxamide (**17d**) (80 mg, 188 μ mol, 0.9 eq) in EtOH (5 mL) was slowly added over a course of 4 h at rt. After 5 h the volatile components were removed under reduced pressure. The residue was used in the next step without further purification or characterisation. LCMS R_f (min) = 2.73. MS m/z 408.2 (M + H).

4-(5-Amino-4-benzoyl-3-(3-(trifluoromethyl)phenyl)thiophen-2-yl)benzoic acid (21a). See literature procedure.¹³

3-(5-Amino-4-benzoyl-3-(3-(trifluoromethyl)phenyl)thiophen-2-yl)benzoic acid (21b). The iodide **20a** (515 mg, 1.00 mmol, 1.0 eq) was dissolved in DMF (6.5 mL) and 3-methoxycarbonylphenyl boronic acid (234 mg, 1.30 mmol) was added, followed by Pd[PPh₃]₂Cl₂ (70 mg, 0.1 mmol, 0.1 eq) and 2 M K₃PO₄ (1.9 mL). The mixture was stirred and heated to 70 °C for 4.5h under an atmosphere of N₂. The cooled solution was slowly diluted with EtOAc (50 mL) and washed with H₂O (4 \times 20 mL) and then followed by brine (20 mL). The organic layer was dried with MgSO₄, filtered and the concentrated to a brown resin (673 mg). The crude material was chromatographed on silica gel (eluent EtOAc: PET 95:5 \rightarrow 80:20) providing the intermediate methyl 3-(5-acetamido-4-benzoyl-3-(3-(trifluoromethyl)phenyl)thiophen-2-yl)benzoate as a yellow solid (350 mg, 67%).

The intermediate Suzuki product (350 mg, 0.657 mmol) was suspended in EtOH: H₂O (6.4 mL, 1:1 ratio). The mixture was added NaOH (263 mg, 6.57 mmol) and stirred on an oil bath (40 °C) for 18 h. The cooled solution was diluted with H₂O (40 mL) and washed with Et₂O (50 mL). The aqueous solution was chilled on an ice bath with stirring and carefully acidified to pH 2 and extracted with EtOAc (50 mL). The organic layer was dried with MgSO₄, filtered and then concentrated providing **21b** as a dark yellow resin (350 mg). LCMS revealed 70% and this crude material was used in the next step without further purification.

2-(5-Amino-4-benzoyl-3-(3-(trifluoromethyl)phenyl)thiophen-2-yl)benzoic acid (21c). The iodide **20a** (515 mg, 1.00 mmol, 1.0 eq) was dissolved in dioxane (12 mL) and H₂O (0.14 mL) and to this mixture was added (2-(methoxycarbonyl)phenyl)boronic acid (270 mg, 1.50 mmol, 1.5 eq) followed by CsF (380 mg, 2.50 mmol, 2.5 eq) and Pd(dppf)·DCM (16 mg, 20.0 μmol, 0.02 eq). The mixture was stirred at rt for 5 min while bubbling N₂ gas through the mixture and then heated to 60 °C for 18 h. The cooled mixture was filtered through a silica plug eluting with Et₂O and then concentrated (632 mg). The crude was chromatographed on silica gel (eluent PET: EtOAc 90:10 → 70:30) providing methyl 2-(5-acetamido-4-benzoyl-3-(3-(trifluoromethyl)phenyl)thiophen-2-yl)benzoate as an amber resin.

The resin was taken up in EtOH (3 mL) and H₂O (3 mL). To the stirring mixture was added NaOH (125 mg, 3.13 mmol) and stirred at rt overnight. The mixture was concentrated to remove EtOH and then diluted with H₂O (40 mL) and washed with Et₂O (2 × 50 mL). The aqueous layer was separated and then acidified to approximately pH 2 with 6 M HCl and extracted with EtOAc (60 mL). The organic layer was dried with MgSO₄, filtered and concentrated to yellow solid (123 mg). The solid was taken up in EtOH and precipitated with H₂O (≈ 70% EtOH mixture) providing **21b** as a yellow solid (92 mg, 31%). ¹H NMR (*d*₆-DMSO) δ 12.75 (s, 1H), 8.11 (s, 2H), 7.70–7.60 (m, 1H), 7.43–7.32 (m, 2H), 7.20–7.04 (m, 5H), 7.01–6.88 (m, 5H); ¹³C NMR (*d*₆-DMSO) δ 191.0, 168.0, 165.9, 140.1, 136.9, 134.2, 133.8, 133.6, 133.1, 132.9, 131.1, 130.0, 129.6, 128.1, 128.1, 128.0, 127.8 (q, *J* = 31.5 Hz), 126.5 (q, *J* = 3.6 Hz), 126.4 (q, *J* = 272.3 Hz), 122.4 (q, *J* = 3.5 Hz), 127.1, 119.6, 113.9.

4-(5-Amino-4-benzoylthiophen-2-yl)benzoic acid (21d). See literature procedure.²³

4-(5-Acetamido-4-benzoyl-3-(3-(trifluoromethyl)phenyl)thiophen-2-yl)benzoic acid (22a). Intermediate **21a** (250 mg, 0.50 mmol, 1.0 eq) in acetic anhydride (2 mL) was heated to 90 °C for 10 min. The resulting solution was cooled to rt then concentrated *in vacuo*. The crude mixture (266 mg) was suspended in THF: distilled H₂O (12 mL, 1:1 ratio) and the flask was purged with N₂.

Solid LiOH (40 mg) was added and the reaction mixture was stirred at rt for 30 min. The THF was removed *in vacuo* at rt. The aqueous solution was diluted with distilled H₂O (30 mL), before being washed with Et₂O (2 x 25 mL). The resulting aqueous solution was cooled to 0 °C and carefully acidified to pH 3 as a yellow precipitate formed. The cooled mixture was stirred for 1 h at low temperature and allowed to settle. The mixture was filtered and washed with cold distilled H₂O, to afford the tilted compound as a yellow solid (249 mg, 98%). ¹H NMR (*d*₆-DMSO) δ 12.98 (s, 1H), 11.00 (s, 1H), 7.78–7.81 (m, 2H), 7.49–7.52 (m, 2H), 7.38–7.42 (m, 2H), 7.20–7.30 (m, 7H), 2.15 (s, 3H); ¹³C NMR (*d*₆-DMSO) δ 192.7, 168.4, 166.8, 142.3, 137.6, 137.2, 135.8, 134.0, 133.3, 132.8, 129.5 (2C), 129.1, (2C), 129.0, 128.7 (q, *J* = 31.8 Hz), 127.1, 128.1, 126.6 (q, *J* = 3.9 Hz), 124.5, 123.8 (q, *J* = 3.6 Hz), 123.7 (q, *J* = 271 Hz), 22.6.

4-(4-Benzoyl-3-(3-(trifluoromethyl)phenyl)thiophen-2-yl)benzoic acid (22b). Intermediate **21a** (660 mg, 1.41 mmol, 1.0 eq) was suspended in anhydrous DMF (4 mL) and added dropwise over 10 min to a heated (63–65 °C) stirring solution of *t*-butylnitrite (250 μL, 2.09 mmol, 1.5 eq) in anhydrous DMF (3 mL). The reaction mixture became dark brown as addition continued, once addition was complete the reaction was stirred for a further 20 min. TLC analysis at this time showed complete consumption of starting material. The reaction mixture was cooled to rt and added dropwise via syringe to ice/water (100 mL). The suspension was stirred for 30 min at low temperature, allowed to settle in the fridge before being filtered. The resulting solid was placed under vacuum overnight before being dry loaded onto a silica column (eluent DCM: MeOH 99:1 → 90:10), concentration of the relevant fraction gave an orange/red solid (584 mg, 91%). ¹H NMR (*d*₆-DMSO) δ 13.07 (s, 1H), 8.23 (s, 1H), 7.87–7.83 (m, 2H), 7.80–7.77 (m, 2H), 7.66–7.57 (m, 3H), 7.51–7.46 (m, 2H), 7.39–7.37 (m, 2H), 7.33–7.30 (m, 2H); ¹³C NMR (*d*₆-DMSO) δ 190.7, 166.8, 141.1, 140.3, 137.3, 137.2, 136.8, 135.8, 134.0, 133.3, 133.2, 130.2, 129.9, 129.6 (2C), 129.3, 128.9 (q, *J* = 28.8 Hz), 126.4 (q, *J* = 3.9 Hz), 124.0 (q, *J* = 3.5 Hz), 123.9 (q, *J* = 270 Hz).

4-(4-Benzoylthiophen-2-yl)benzoic acid (22c). 4-(5-Amino-4-benzoylthiophen-2-yl)benzoic acid (**21d**) (300 mg, 928 μ mol, 1.0 eq) was dissolved in DMF (30 mL) and *tert*-butylnitrite (219 μ L, 1.86 mmol, 2.0 eq) was added. The mixture was heated to 60 °C for 1.5 h then allowed to cool to rt. The mixture was diluted with H₂O (90 mL) and red/brown precipitate formed. The precipitate was collected and washed thoroughly with H₂O and suck dried (205 mg, 72%). ¹H NMR (*d*₆-DMSO) δ 13.07 (br s, 1H), 8.33–8.27 (m, 1H), 8.04–7.97 (m, 3H), 7.92–7.83 (m, 4H), 7.73–7.67 (m, 1H), 7.62–7.56 (m, 2H). This material was sufficiently pure to use in the next step.

Methyl 4-(3-bromothiophen-2-yl)benzoate (24a). 2,3-Dibromothiophene (**31b**) (566 μ L, 5.00 mmol, 1.0 eq) was dissolved in DMF (40 mL) and to this mixture was added 2 M K₃PO₄ (10 mL) followed by (4-(methoxycarbonyl)phenyl)boronic acid (1.08 g, 6.00 mmol, 1.2 eq) and Pd[PPh₃]₂Cl₂ (35 mg, 0.05 mmol, 0.1 eq). The mixture was stirred at rt for 5 min while bubbling N₂ gas through the mixture. The mixture was then heated to 80 °C for 16 h. The cooled mixture was partitioned between Et₂O (100 mL) and H₂O (100 mL). The aqueous layer was extracted with Et₂O (50 mL) and the combined organic layers were washed with brine (50 mL) and then dried with MgSO₄, filtered and concentrated to a solid (1.22 g). The crude material was chromatographed on silica gel (eluent Et₂O: PET 10:90) providing **24a** (519 mg, 35%). ¹H NMR (CDCl₃) δ 8.09 (d, *J* = 8.3 Hz, 2H), 7.75 (d, *J* = 8.3 Hz, 2H), 7.34 (d, *J* = 5.3 Hz, 1H), 7.09 (d, *J* = 5.3 Hz, 1H), 3.94 (s, 3H); ¹³C NMR (CDCl₃) δ 166.8, 137.5, 137.1, 132.3, 129.9, 129.8, 129.0, 126.1, 108.7, 52.4.

Methyl 4-(5-amino-4-benzoylthiophen-2-yl)benzoate (24b). 2-Iodothiophene (**23b**) (0.51 mL, 5.0 mmol, 1.0 eq) was dissolved in DMF (40 mL) and to this mixture was added 2 M K₃PO₄ (10 mL) followed by (4-(methoxycarbonyl)phenyl)boronic acid (1.35 g, 7.5 mmol, 1.5 eq) and Pd[PPh₃]₂Cl₂ (70 mg, 0.10 mmol, 0.1 eq). The mixture was stirred at rt for 5 min while bubbling N₂ gas through the mixture. The mixture was then heated to 80 °C for 16 h. The cooled mixture was partitioned between EtOAc (100 mL) and H₂O (100 mL). The aqueous layer was extracted with EtOAc (50 mL) and the combined organic layers were washed with H₂O (2 \times 50 mL) and

finally with brine (50 mL) and then dried with MgSO_4 , filtered and concentrated to a pale yellow solid (1.2 g). The crude material was recrystallised from EtOH providing **24b** as a pale yellow solid (832 mg, 76%). ^1H NMR (CDCl_3) δ 8.04 (d, J = 8.4 Hz, 2H), 7.67 (d, J = 8.4 Hz, 2H), 7.42 (dd, J = 3.6, 0.9 Hz, 1H), 7.36 (dd, J = 5.1, 0.9 Hz, 1H), 7.11 (dd, J = 5.0, 3.7 Hz, 1H), 3.93 (s, 3H); ^{13}C NMR (CDCl_3) δ 166.9, 143.2, 138.8, 130.4, 128.9, 128.4, 126.4, 125.6, 124.6, 52.2.

Methyl 4-(thiophen-2-yl)benzoate (25). Methyl 4-(thiophen-2-yl)benzoate (**24b**) (275 mg, 1.26 mmol, 1.0 eq) was taken up in EtOH (7.5 mL) and H_2O (7.5 mL). To the stirring mixture was added $\text{LiOH}\cdot\text{H}_2\text{O}$ (159 mg, 3.78 mmol, 3.0 eq) and stirred at rt overnight. The mixture was concentrated to remove EtOH and then diluted with H_2O (70 mL) and washed with Et_2O (50 mL). The aqueous layer was separated and then acidified to approximately pH 2 with 6 M HCl precipitating a powder that was thoroughly washed with H_2O (138 mg). The solid was recrystallised from CHCl_3 to provide **25** as an off-white solid (70 mg, 27%). ^1H NMR (d_6 -DMSO) δ 12.99 (br s, 1H), 7.96 (d, J = 8.3 Hz, 2H), 7.79 (d, J = 8.3 Hz, 2H), 7.69–7.62 (m, 2H), 7.19 (dd, J = 4.9, 3.8 Hz, 1H).

Methyl 4-(3-(3-(trifluoromethyl)phenyl)thiophen-2-yl)benzoate (26). Methyl 4-(3-bromothiophen-2-yl)benzoate (**24a**) (519 mg, 1.75 mmol, 1.0 eq) was dissolved in DMF (14 mL) and to this mixture was added 2 M K_3PO_4 (3.5 mL) followed by (3-(trifluoromethyl)phenyl)boronic acid (498 mg, 2.62 mmol, 1.5 eq) and $\text{Pd}[\text{PPh}_3]_2\text{Cl}_2$ (35 mg, 0.05 mmol, 0.1 eq). The mixture was stirred at rt for 5 min while bubbling N_2 gas through the mixture. The mixture was then heated to 80 °C for 18 h. The cooled mixture was partitioned between Et_2O (100 mL) and H_2O (100 mL). The aqueous layer was extracted with Et_2O (50 mL) and the combined organic layers were washed H_2O (2×50 mL) and finally with brine (50 mL) and then dried with MgSO_4 , filtered and concentrated to a viscous oil 679 mg. The crude material was chromatographed on silica gel (eluent Et_2O : PET 5:95 \rightarrow 10:90) providing **26** as clear resin (404 mg, 64%). ^1H NMR (CDCl_3) δ 7.94 (d, J = 8.7 Hz, 2H), 7.60–7.49 (m, 2H), 7.43 (d, J = 5.2 Hz, 1H), 7.41–7.36 (m, 2H), 7.33 (d, J = 8.6

Hz, 2H), 7.19 (d, $J = 5.2$ Hz, 1H), 3.91 (s, 3H); ^{13}C NMR (CDCl_3) δ 166.8, 138.5, 137.7, 137.1, 132.6, 132.6, 131.1 (q, $J = 32.3$ Hz), 130.5, 130.0, 129.3, 129.2, 129.1, 126.1–125.7 (m), 125.9, 124.1 (q, $J = 272.4$ Hz), 124.0 (q, $J = 3.7$ Hz), 52.3.

4-(3-(3-(Trifluoromethyl)phenyl)thiophen-2-yl)benzoic acid (27). Methyl 4-(3-(3-(trifluoromethyl)phenyl)thiophen-2-yl)benzoate (**26**) (400 mg, 1.10 mmol, 1.0 eq) was dissolved in EtOH (15 mL) and H_2O (5 mL). To the stirring mixture was added NaOH (200 mg, 5.0 mmol, 4.5 eq) and stirred at rt for 5 h. The mixture was concentrated to remove EtOH and then diluted with H_2O (50 mL) and then acidified to approximately pH 2 with 6 M HCl and then extracted with DCM (2×50 mL). The combined organics were dried with MgSO_4 , filtered and concentrated to provide **27** as a pale yellow coloured solid (318 mg, 83%). ^1H NMR (CDCl_3) δ 8.05 (d, $J = 6.9$ Hz, 2H), 7.65–7.53 (m, 2H), 7.53–7.37 (m, 5H), 7.29–7.21 (m, 1H); ^{13}C NMR (CDCl_3) δ 171.9, 139.5, 138.4, 138.0, 137.1, 132.6, 130.7, 130.6, 131.2 (q, $J = 32.3$ Hz), 129.4, 129.2, 128.4, 126.1 125.9 (q, $J = 3.8$ Hz), 124.1 (q, $J = 3.9$ Hz), 124.1 (q, $J = 272$ Hz).

Benzyl 5-bromothiophene-2-carboxylate (29a). 5-Bromothiophene-2-carboxylic acid **28a** (1.00 g, 4.83 mmol, 1.0 eq) was dissolved in DMF (20 mL) and to this mixture was added Cs_2CO_3 (3.26 g, 10.0 mmol, 2.1 eq), TBAI (178 mg, 483 μmol , 0.1 eq) and the mixture was allowed to stir at rt for 10 min. Finally BnBr (606 μL , 5.10 mmol, 1.1 eq) was added to the stirring mixture and allowed to stir at rt for 20 h. The mixture was diluted with MTBE (50 mL) and washed with H_2O (3×50 mL) and finally with brine (20 mL). The organic layer was dried with MgSO_4 , filtered and then concentrated to a residue that was chromatographed on silica gel (eluent PET: EtOAc 100:0 \rightarrow 0:100) **29a** as a clear colourless oil (1.41 g, 98%). ^1H NMR (CDCl_3) δ 7.58 (d, $J = 4.0$ Hz, 1H), 7.44–7.34 (m, 5H), 7.07 (d, $J = 4.0$ Hz, 1H), 5.32 (s, 2H).

Benzyl 4-bromothiophene-2-carboxylate (29b). 4-Bromothiophene-2-carboxylic acid (**28b**) (1.00 g, 4.83 mmol, 1.0 eq) was dissolved in DMF (20 mL) and to this mixture was added Cs_2CO_3 (3.26 g, 10.0 mmol, 2.0 eq), TBAI (178 mg, 483 μmol , 0.1 eq) and the mixture was allowed to stir

at rt for 10 min. Finally, BnBr (606 μ L, 5.10 mmol, 1.1 eq) was added to the stirring mixture and allowed to stir at rt for 20 h. The mixture was diluted with MTBE (50 mL) and washed with H₂O (3 \times 50 mL) and finally with brine (20 mL). The organic layer was dried with MgSO₄, filtered and then concentrated to a residue that was chromatographed on silica gel (eluent PET: EtOAc 100: \rightarrow 90:10) providing **29b** as a clear colourless oil (1.42 g, 98%). ¹H NMR (CDCl₃) δ 7.71 (d, J = 1.5 Hz, 1H), 7.45 (s, 1H), 7.44–7.34 (m, 5H), 5.33 (s, 2H).

Benzyl 4-(3-(trifluoromethyl)phenyl)thiophene-2-carboxylate (29c). Benzyl 4-bromothiophene-2-carboxylate (**29b**) (1.40 g, 4.71 mmol, 1.0 eq) was dissolved in dioxane (38 mL) and H₂O (440 μ L) and to this mixture was added (3-(trifluoromethyl)phenyl)boronic acid (1.10 g, 6.12 mmol, 1.5 eq) followed by CsF (1.43 g, 9.42 mmol, 2.0 eq) and Pd(dppf)DCM (192 mg, 236 μ mol, 0.05 eq). The mixture was stirred at rt for 5 min while bubbling N₂ gas through the mixture and then heated to 60 $^{\circ}$ C for 5 h. The cooled mixture was diluted with MTBE (50 mL) and washed with H₂O (3 \times 50 mL) and finally with brine (20 mL). The organic layer was dried with MgSO₄, filtered and then concentrated to a dark brown oil (2.52 g). The oil was chromatographed on silica gel (eluent PET: EtOAc 100:0 \rightarrow 90:10) providing **29c** as a clear colourless oil (1.22 g, 66%). ¹H NMR (CDCl₃) δ 8.11 (d, J = 1.6 Hz, 1H), 7.84–7.81 (m, 1H), 7.76–7.72 (m, 1H), 7.71 (d, J = 1.6 Hz, 1H), 7.61–7.57 (m, 1H), 7.55–7.47 (m, 3H), 7.46–7.35 (m, 3H), 5.40 (s, 2H); ¹³C NMR (CDCl₃) δ 161.9, 141.4, 135.7, 135.5, 134.9, 132.0, 131.4 (q, J = 32.3 Hz), 129.6, 129.5, 128.8, 128.5, 128.4, 128.1, 124.4 (q, J = 3.7 Hz), 124.1 (q, J = 272.3 Hz), 123.1 (q, J = 3.8 Hz), 67.1.

Benzyl 5-bromo-4-(3-(trifluoromethyl)phenyl)thiophene-2-carboxylate (29d). Benzyl 4-(3-(trifluoromethyl)phenyl)thiophene-2-carboxylate (**29c**) (1.22 g, 3.36 mmol, 1.0 eq) was dissolved in AcOH (10 mL) and NBS (629 mg, 3.53 mmol, 1.1 eq) was added to the mixture. The mixture was heated to 60 $^{\circ}$ C for 2 h and then allowed to cool to rt and then diluted with Et₂O (100 mL). The mixture was washed with saturated bicarbonate (2 \times 50 mL) and finally with brine (50 mL). The organic layer was dried with MgSO₄, filtered and concentrated to provide **29d** as an amber resin

(1.57 g, 100%). ^1H NMR (CDCl_3) δ 7.81–7.62 (m, 4H), 7.61–7.53 (m, 1H), 7.47–7.32 (m, 5H), 5.35 (s, 2H). This material was sufficiently pure to use directly in the next step.

Benzyl 5-(4-(methoxycarbonyl)phenyl)thiophene-2-carboxylate (30a). Benzyl 5-bromothiophene-2-carboxylate (**29a**) (1.40 g, 4.71 mmol, 1.0 eq) was dissolved in dioxane (38 mL) and H_2O (440 μL) and to this mixture was added (4-(methoxycarbonyl)phenyl)boronic acid (1.10 g, 6.12 mmol, 1.5 eq) followed by CsF (1.43 g, 9.42 mmol, 2.0 eq) and $\text{Pd}(\text{dppf})\text{DCM}$ (192 mg, 236 μmol , 0.05 eq). The mixture was stirred at rt for 5 min while bubbling N_2 gas through the mixture and then heated to 60 $^\circ\text{C}$ for 18 h. The cooled mixture was diluted with MTBE (50 mL) and washed with H_2O (3×50 mL) and finally with brine (20 mL). The organic layer was dried with MgSO_4 , filtered and then concentrated to a brown solid (2.11 g). The solid was chromatographed on silica gel (eluent DCM 100%) providing **30a** as a beige coloured solid (1.26 g, 76%). ^1H NMR (CDCl_3) δ 8.06 (d, $J = 8.2$ Hz, 2H), 7.81 (d, $J = 3.9$ Hz, 1H), 7.69 (d, $J = 8.2$ Hz, 2H), 7.51–7.31 (m, 6H), 5.36 (s, 2H), 3.93 (s, 3H); ^{13}C NMR (CDCl_3) δ 166.6, 161.9, 149.9, 137.6, 135.8, 134.7, 133.5, 130.5, 130.2, 128.8, 128.5, 128.3, 126.1, 125.0, 67.0, 52.4.

Benzyl 5-(4-(methoxycarbonyl)phenyl)-4-(3-(trifluoromethyl)phenyl)thiophene-2-carboxylate (30b). Intermediate **29d** (1.57 g, 3.56 mmol, 1.0 eq) was dissolved in dioxane (29 mL) and H_2O (333 μL) and to this mixture was added (4-(methoxycarbonyl)phenyl)boronic acid (1.10 g, 6.12 mmol, 2.0 eq) followed by CsF (2.10 g, 13.9 mmol, 4.0 eq) and $\text{Pd}(\text{dppf})\text{DCM}$ (58 mg, 71.6 μmol , 0.05 eq). The mixture was stirred at rt for 5 min while bubbling N_2 gas through the mixture and then heated to 60 $^\circ\text{C}$ for 18 h. The cooled mixture was diluted with MTBE (100 mL) and washed with H_2O (3×70 mL) and finally with brine (50 mL). The organic layer was dried with MgSO_4 , filtered and then concentrated to an amber coloured semi-solid (2.12 g). The crude was chromatographed on silica gel (eluent PET: EtOAc 100:0 \rightarrow 90:10) providing **30b** as a clear colourless resin (1.48 g, 84%). ^1H NMR (CDCl_3) δ 7.96 (d, $J = 8.6$ Hz, 2H), 7.87 (s, 1H), 7.58–7.52 (m, 2H), 7.49–7.43 (m, 2H), 7.43–7.32 (m, 6H), 5.38 (s, 2H), 3.91 (s, 3H).

5-(4-(Methoxycarbonyl)phenyl)thiophene-2-carboxylic acid (31a). Intermediate **30a** (700 mg, 1.99 mmol) was suspended in EtOAc (30 mL) and DMF (20 mL) in an N₂ atmosphere followed by 10% Pd/C (120 mg). The flask was evacuated and flushed with H₂ gas three times and then stirred in an H₂ atmosphere for 4 days at rt. The mixture was filtered through CeliteTM and diluted with EtOAc (100 mL) and washed with H₂O (3 × 50 mL), dried with MgSO₄, filtered and then concentrated to provide **31a** as a white solid (427 mg, 82%). ¹H NMR (CDCl₃) δ 8.07 (d, *J* = 8.6 Hz, 2H), 7.82 (d, *J* = 4.0 Hz, 1H), 7.70 (d, *J* = 8.6 Hz, 2H), 7.39 (d, *J* = 3.9 Hz, 1H), 3.94 (s, 3H).

5-(4-(Methoxycarbonyl)phenyl)-4-(3-(trifluoromethyl)phenyl)thiophene-2-carboxylic acid (31b). Intermediate **30b** (1.48 g, 2.98 mmol, 1.0 eq) was suspended in EtOAc (30 mL) and *i*PrOH (20 mL) in an N₂ atmosphere followed by 10% Pd/C (200 mg). The mixture evacuated and flushed with H₂ gas three times and then stirred in an H₂ atmosphere for 18h. The mixture was filtered through CeliteTM and concentrated to provide **31b** as a clear colourless resin (1.08 g, 89%). ¹H NMR (CDCl₃) δ 7.99 (d, *J* = 8.6 Hz, 2H), 7.96 (s, 1H), 7.61–7.54 (m, 2H), 7.45–7.34 (m, 4H), 3.93 (s, 3H).

Methyl 4-(5-((tert-butoxycarbonyl)amino)thiophen-2-yl)benzoate (32a). Intermediate **31a** (420 mg, 1.60 mmol, 1.0 eq) was taken up in *tert*-BuOH (20 mL) and DPPA (381 μL, 1.76 mmol, 1.1 eq) was added followed by Et₃N (258 μL, 1.85 mmol, 1.2 eq). The mixture was refluxed for 5 h and then cooled to rt and concentrated to a residue. The residue was taken up in Et₂O (60 mL) and washed with H₂O (3 × 50 mL) and finally with brine (30 mL), dried with MgSO₄, filtered and concentrated to a yellow solid (729 mg). The crude solid was chromatographed on silica gel (eluent DCM 100%) providing **32a** as a yellow coloured solid (366 mg, 69%). ¹H NMR (CDCl₃) δ 7.99 (d, *J* = 8.7 Hz, 2H), 7.60 (d, *J* = 8.6 Hz, 2H), 7.16 (d, *J* = 4.0 Hz, 1H), 7.04 (s, 1H), 6.49 (d, *J* = 4.0 Hz, 1H), 3.91 (s, 3H), 1.55 (s, 9H).

Methyl 4-(5-((tert-butoxycarbonyl)amino)-3-(3-(trifluoromethyl)phenyl)thiophen-2-yl)benzoate (32b). Intermediate **31b** (1.08 g, 2.66 mmol, 1.0 eq) was taken up in *tert*-BuOH (50

mL) and DPPA (632 μ L, 2.92 mmol, 1.1 eq) was added followed by Et₃N (444 μ L, 3.19 mmol, 1.2 eq). The mixture was refluxed for 5 h and then cooled to rt and concentrated to a residue. The residue was taken up in Et₂O (100 mL) and washed with H₂O (3 \times 50 mL) and finally with brine (30 mL), dried with MgSO₄, filtered and concentrated to a yellow residue (1.4 g). The crude was chromatographed on silica gel (eluent PET: EtOAc 95:5 \rightarrow 90:10) providing **32b** as a yellow coloured solid (907 mg, 71% yield). ¹H NMR (CDCl₃) δ 7.89 (d, J = 8.6 Hz, 2H), 7.58–7.48 (m, 2H), 7.40–7.34 (m, 2H), 7.29 (d, J = 8.6 Hz, 2H), 7.06 (br s, 1H), 6.59 (s, 1H), 3.89 (s, 3H), 1.55 (s, 9H).

4-(5-((*tert*-Butoxycarbonyl)amino)thiophen-2-yl)benzoic acid (33a). Intermediate **32a** (360 mg, 1.08 mmol, 1.0 eq) was taken up in a mixture of dioxane (10 mL), EtOH (10 mL) and H₂O (8 mL) and 2 M NaOH (4.0 mL, 8.0 mmol, 7.4 eq) and stirred at rt for 3 days. The mixture was concentrated to a residue and then dissolved in H₂O (5 mL) and washed with Et₂O (10 mL). The aqueous layer was acidified with 10% citric acid (\approx pH 3-4) and extracted with EtOAc (2 \times 20 mL). The combined organic extracts were dried with MgSO₄, filtered and then concentrated to provide **32a** as an amber coloured solid (292 mg, 85%). ¹H NMR (*d*₆-DMSO) δ 12.83 (br s, 1H), 10.67 (br s, 1H), 7.90 (d, J = 8.3 Hz, 2H), 7.65 (d, J = 8.4 Hz, 2H), 7.37 (d, J = 4.0 Hz, 1H), 6.54 (d, J = 4.0 Hz, 1H), 1.49 (s, 9H).

4-(5-((*tert*-Butoxycarbonyl)amino)-3-(3-(trifluoromethyl)phenyl)thiophen-2-yl)benzoic acid (33b). Intermediate **32b** (900 mg, 1.89 mmol, 1.0 eq) was taken up in a mixture of dioxane (10 mL), EtOH (10 mL) and 2 M NaOH (7.55 mL, 15.1 mmol, 8.0 eq) and stirred at rt for 18 h. The mixture was concentrated to a solid residue and then dissolved in H₂O (20 mL) and washed with Et₂O (10 mL). The aqueous layer was acidified with 10% citric acid (\approx pH 3-4) and extracted with EtOAc (3 \times 100 mL). The combined organic extracts were dried with MgSO₄, filtered and then concentrated to provide **33b** as an off-white/peach coloured solid (855 mg, 98%). ¹H NMR

(CDCl₃) δ 7.95 (d, J = 8.5 Hz, 2H), 7.60–7.49 (m, 2H), 7.41–7.36 (m, 2H), 7.32 (d, J = 8.6 Hz, 2H), 7.09 (br s, 1H), 6.60 (s, 1H), 1.56 (s, 9H).

4-(5-Aminothiophen-2-yl)benzoic acid hydrochloride (34a). Intermediate **33a** (100 mg, 313 μ mol) was dissolved in 4 M HCl in dioxane (4 mL) and stirred at rt overnight. The mixture was concentrated and the crude solid was triturated in EtOH (4 mL) and the solid collected and washed with EtOAc and finally Et₂O providing the hydrochloride salt **34a** as a yellow/brown solid (70 mg, 87%). ¹H NMR (*d*₆-DMSO) δ 7.84 (d, J = 7.0 Hz, 2H), 7.51 (d, J = 7.1 Hz, 2H), 7.26 (dd, J = 3.6, 1.3 Hz, 1H), 6.11 (d, J = 2.5 Hz, 1H).

4-(5-Amino-3-(3-(trifluoromethyl)phenyl)thiophen-2-yl)benzoic acid (34b). 4-(5-((*tert*-butoxycarbonyl)amino)-3-(3-(trifluoromethyl)phenyl)thiophen-2-yl)benzoic acid (**33b**) (320 mg, 690 μ mol) was dissolved in EtOAc (3 mL) and 4 M HCl in dioxane (5 mL) was added to the mixture which was stirred at rt for 4 h. The mixture was evaporated to provide a brown solid (280 mg, 100%). ¹H NMR (*d*₆-DMSO) δ 7.76 (d, J = 8.5 Hz, 2H), 7.68–7.61 (m, 1H), 7.60–7.45 (m, 3H), 7.16 (d, J = 8.4 Hz, 2H), 6.14 (s, 1H).

Pharmacology. Materials. Dulbecco's Modified Eagle Medium (DMEM), trypsin and Fluo-4 were purchased from Invitrogen (Carlsbad, CA). Hygromycin-B was purchased from Roche (Basel, Switzerland). Fetal bovine serum (FBS) was purchased from ThermoTrace (Melbourne, Australia). AlphaScreen LANCE cAMP kit was purchased from PerkinElmer (Waltham, MA). VCP746 was synthesized in-house as described previously.¹³ All other reagents were purchased from Sigma-Aldrich (St. Louis, MO) and were of analytical quality.

Cell culture. Chinese hamster ovary FlpIn (FlpIn-CHO) cells stably expressing the human A₁AR, A_{2A}AR, A_{2B}AR or A₃AR were generated as described previously.³⁵ FlpIn-CHO cells were grown in DMEM containing 10% v/v FBS and maintained at 37°C in a humidified incubator

containing 5% CO₂. Adenosine receptor expression was maintained by regular exposure to the selection antibiotic hygromycin-B (500 µg/mL). For cAMP assays, cells were suspended in DMEM containing 10% v/v FBS and seeded into 96-well culture plates at a density of 2 x 10⁴ cells/well. Cells were maintained for 16-18 h at 37°C in a humidified incubator containing 5% CO₂ prior to assay. For calcium mobilization assays, cells were suspended in DMEM containing 10% v/v FBS and seeded into 96-well culture plates at a density of 4 x 10⁴ cells/well. After 6 h, cells were washed once with serum free DMEM and maintained in serum free DMEM for 16-18 h at 37°C in a humidified incubator containing 5% CO₂ prior to assay.

cAMP assays. Media was removed and cells were incubated with cAMP stimulation buffer (140 mM NaCl, 5 mM KCl, 0.8 µM MgSO₄, 0.2 mM Na₂HPO₄, 0.44 mM KH₂PO₄, 1.3 mM CaCl₂, 5.6 mM D-glucose, 5 mM HEPES, 0.1% BSA, 1 U/mL ADA and 10 µM rolipram, pH 7.45), for 1 h incubation at 37°C. Following the 1 h incubation, cells were exposed to agonist in the absence or presence of forskolin. Inhibition of cAMP accumulation mediated by the A₁AR and A₃AR involved agonist treatment of cells for 10 min, followed by the addition of forskolin (3 µM) and incubation for an additional 30 min at 37°C. Stimulation of cAMP accumulation mediated by the A_{2A}AR and A_{2B}AR involved agonist treatment of cells for 40 min at 37°C. Stimulation was terminated by removal of cAMP stimulation buffer and addition of 50 µL/well ice-cold 100% ethanol. Following evaporation of the ethanol, 50 µL/well cAMP lysis buffer (0.1% BSA, 0.3% Tween-20 and 5 mM HEPES, pH 7.4) was added and plates were agitated for 10 min. Detection was performed using an Alphascreen LANCE cAMP kit, as described previously.³⁶ Concentration-response curves were normalized to the baseline response (0%) mediated by 3 µM forskolin (A₁-FlpInCHO and A₃-FlpInCHO) or buffer (A_{2A}-FlpInCHO and A_{2B}-FlpInCHO) and the maximal response (100%) mediated by buffer (A₁-FlpInCHO and A₃-FlpInCHO) or 10 µM forskolin (A_{2A}-FlpInCHO and A_{2B}-FlpInCHO).

Calcium mobilization assay. A₁AR-mediated calcium mobilization was performed as described previously.¹⁹ Briefly, media was removed and replaced with HEPES-buffered saline solution (10 mM HEPES, 146 mM NaCl, 10 mM D-glucose, 5 mM KCl, 1 mM MgSO₄, 1.3 mM CaCl₂, and 1.5 mM NaHCO₃, pH 7.45) containing 1 U/mL of ADA, 2.5 mM probenecid, 0.5% bovine serum albumin (BSA) and 1 μM Fluo-4. Plates were incubated in the dark for 1 h at 37°C, after which addition of agonist and determination of fluorescence was assessed with a FlexStation plate reader (Molecular Devices, Sunnyvale, CA, USA). Concentration-response data were normalized to the response mediated by adenosine triphosphate (ATP; 100 μM).

Data analysis. Statistical analyses and curve fitting were performed using Prism 7 (GraphPad Software, San Diego, CA). To derive potency estimates, concentration-response data were fitted to a three-parameter Hill equation, as described previously.¹⁹ Signaling bias was quantified by fitting concentration-response data to a re-parameterization of the operational model of agonism, as described in detail previously.¹⁹ All results are expressed as the mean ± standard error of the mean (SEM). Statistical analysis involved an unpaired t-test or one-way analysis of variance (ANOVA) with a Dunnett's post-hoc test.

Molecular Modelling. *Homology Modelling of A₁AR.* The sequence of the human A₁AR was retrieved from the Swiss-Prot database. MODELLER software (version 9.18)³⁷ was used to align the A₁AR sequence and built the three-dimensional structure of A₁AR based on the crystal structure of the adenosine A_{2A} receptor (A_{2A}AR) bound to an engineered G protein (PDB ID: 5G53).³² Several extracellular loop features present in the A₁AR inactive crystal structure (PDB ID: 5UEN)³⁰ such as the conserved disulfide bond between residue C80^{3,25} at the top of TM3 and C169^{ECL2}, the ECL3 intraloop disulfide bond between C260^{ECL3} and C263^{ECL3}, the alpha helices formed by ECL2 residues (148-161 and 171-174), and a short beta sheet between ECL1 residues 75-77 and ECL2 residues 165-167 were built and maintained as a constraint for geometric optimization. The best

structure was selected based on the MODELLER Discrete Optimized Protein Energy assessment score and visual inspection.

Docking of Adenosine and 1. Docking of Adenosine and VCP746 was performed using ICM software (version 3.8.5; Molsoft LLC, San Diego, CA). The receptor was first converted to an ICM object using the molecular conversion procedure, implemented in ICM. This procedure adds hydrogen atoms to the PDB receptor structure and flips His, Asn, and Gln side chains to improve molecular interactions and performs a global optimization of the hydrogens to find the best hydrogen-bonding network. Potential binding sites were predicted using the ICM Pocket Finder algorithm.^{38,39} Docking search boundaries (the region in which 0.5-Å grid energy maps were generated) was set as default. Docking thoroughness (representing the length of the docking simulation), were set as 5. No distance restraints were used in the adenosine docking procedure. Compound **1** was docked using the template docking method where the adenosine moiety of **1** was constrained to the position of adenosine in the receptor. Ligand binding modes were ranked according to ICM score, which is inversely proportional to the number of favorable intermolecular interactions between the docked ligand and the receptor. The docking of each ligand was repeated three times and the model with the most favorable combination of ICM binding score and conformation of the adenosine moiety, compared to the adenosine bound A_{2A}AR crystal structure (PDB ID: 2YDO), was selected. The generalized numbering scheme proposed by Ballesteros and Weinstein was used for transmembrane residues.⁴⁰ All figures were generated with PYMOL.

■ AUTHOR INFORMATION

Corresponding Authors

*For P.J.S.: phone: +613 9903 9542; E-mail: peter.scammells@monash.edu.

*For L.T.M.: phone: +613 9903 9095; E-mail: lauren.may@monash.edu.

Author Contributions

The manuscript was written through contributions of all authors, and all authors have given approval to the final version of the manuscript.

Notes

The authors declare no competing financial interest.

■ ACKNOWLEDGMENTS

This work was funded by Project Grant APP1084487 of the National Health and Medical Research Council of Australia (NHMRC). A.C. is a Senior Principal Research Fellow of the NHMRC. L.T.M. is a recipient of an Australian Research Council Discovery Early Career Researcher Award. J-A.B. is a recipient of an Australian Government Research Training Program Scholarship.

■ ABBREVIATIONS

AcOH, acetic acid; ANOVA, one-way analysis of variance; AR, adenosine receptor; ATP, adenosine triphosphate; Boc, *tert*-butyloxycarbonyl; BOP, (benzotriazol-1-yloxy)tris(dimethylamino)phosphonium hexafluorophosphate; BSA, bovine serum albumin; cat, catalytic; CHCl₃, chloroform; DCM, dichloromethane; DMEM, Dulbecco's Modified Eagle Medium; DMF, *N,N*-dimethylformamide; DPPA, diphenylphosphoryl azide; eq, equivalent; Et₂O, diethyl ether; EtOAc, ethyl acetate; EtOH, ethanol; FBS, Fetal bovine serum; FCC, flash column chromatography; FlpIn-CHO, Chinese hamster ovary cells with FlpIn vector; HRMS, high resolution mass spectrometry; *i*PrOH, isopropyl alcohol; LCMS, liquid chromatography mass spectrometry; MeOH, methanol; MgSO₄, magnesium sulfate; MTBE, methyl *tert*-butyl ether; Na₂SO₄, sodium sulfate; NH₄OH, ammonium hydroxide; NMR, nuclear magnetic resonance; PET,

petroleum spirits 40-60; rt, room temperature; SEM, Standard error of the mean; *tert*-BuOH, tertiary butanol; TBAI, tetrabutylammonium iodide ; THF, tetrahydrofuran.

■ ASSOCIATED CONTENT

Supporting Information

The Supporting Information is available free of charge on the ACS Publications website:

Details of the synthesis of intermediate **16d**

Molecular formula strings

Atomic coordinates of the homology model

■ REFERENCES

(1) Fredholm, B. B.; IJzerman, A. P.; Jacobson, K. A.; Linden, J.; Müller, C. E. International union of basic and clinical pharmacology. LXXXI. Nomenclature and classification of adenosine receptors - an update. *Pharmacol. Rev.* **2011**, *63*, 1–34.

(2) Fredholm, B. B.; IJzerman, A. P.; Jacobson, K. A.; Klotz, K.-N.; Linden, J. International Union of Pharmacology. XXV. Nomenclature and Classification of Adenosine Receptors. *Pharmacol. Rev.* **2001**, *53*, 527–552.

(3) Imlach, W. L.; Bhola, R. F.; May, L. T.; Christopoulos, A.; Christie, M. J. A Positive Allosteric Modulator of the Adenosine A₁ Receptor Selectively Inhibits Primary Afferent Synaptic Transmission in a Neuropathic Pain Model. *Mol Pharmacol.* **2015**, *88*, 460–468.

(4) Luongo, L.; Guida, F.; Imperatore, R.; Napolitano, F.; Gatta, L.; Cristino, L.; Giordano, C.; Siniscalco, D.; Di, M. V.; Bellini, G.; Petrelli, R.; Cappellacci, L.; Usiello, A.; de, N. V.; Rossi, F.; Maione, S. The A₁ Adenosine Receptor as a New Player in Microglia Physiology. *Glia* **2014**, *62*, 122-132.

- (5) Müller, C. E.; Jacobson, K. A. Recent Developments in Adenosine Receptor Ligands and their Potential as Novel Drugs. *Biochim. Biophys. Acta, Biomembr.* **2011**, *1808*, 1290–1308.
- (6) Gao, Z.-G.; Jacobson, K. A. Emerging Adenosine Receptor Agonists - an Update. *Expert Opin. Emerg. Drugs* **2011**, *16*, 597–602.
- (7) Headrick, J. P.; Ashton, K. J.; Rose'Meyer, R. B.; Peart, J. N. Cardiovascular Adenosine Receptors: Expression, Actions and Interactions. *Pharmacol. Ther.* **2013**, *140*, 92–111.
- (8) Yang, Z.; Cerniway, R. J.; Byford, A. M.; Berr, S. S.; French, B. A.; Matherne, G. P. Cardiac Overexpression of A₁-Adenosine Receptor Protects Intact Mice Against Myocardial Infarction. *Am. J. Physiol.* **2002**, *282*, H949–H955.
- (9) Shryock, J. C.; Belardinelli, L. Adenosine and Adenosine Receptors in the Cardiovascular System: Biochemistry, Physiology, and Pharmacology. *Am. J. Cardiol.* **1997**, *79*, 2–10.
- (10) Ross, A. M.; Gibbons, R. J.; Stone, G. W.; Kloner, R. A.; Alexander, R. W. A Randomized, Double-blinded, Placebo-controlled Multicenter Trial of Adenosine as an Adjunct to Reperfusion in the Treatment of Acute Myocardial Infarction (AMISTAD-II). *J. Am. Coll. Cardiol.* **2005**, *45*, 1775–1780.
- (11) Belardinelli, L.; Shryock, J. C.; Song, Y.; Wang, D.; Srinivas, M. Ionic Basis of the Electrophysiological Actions of Adenosine on Cardiomyocytes. *FASEB J.* **1995**, *9*, 359–365.
- (12) Violin, J. D.; Lefkowitz, R. J. β -Arrestin-biased Ligands at Seven-transmembrane Receptors. *Trends Pharmacol. Sci.* **2007**, *28*, 416–422.
- (13) Valant, C.; May, L. T.; Aurelio, L.; Chuo, C. H.; White, P. J.; Baltos, J.-A.; Sexton, P. M.; Scammells, P. J.; Christopoulos, A. Separation of On-target Efficacy from Adverse Effects through Rational Design of a Bitopic Adenosine Receptor Agonist. *Proc. Natl. Acad. Sci. U. S. A.* **2014**, *111*, 4614–4619.
- (14) Marti-Solano, M.; Guixa-Gonzalez, R.; Sanz, F.; Pastor, M.; Selent, J. Novel Insights into Biased Agonism at G Protein-Coupled Receptors and their Potential for Drug Design. *Curr. Pharm. Des.* **2013**, *19*, 5156–5166.

(15) Kenakin, T.; Christopoulos, A. Signalling Bias in New Drug Discovery: Detection, Quantification and Therapeutic Impact. *Nat. Rev. Drug Discov.* **2013**, *12*, 205–216.

(16) Kenakin, T. The Potential for Selective Pharmacological Therapies through Biased Receptor Signaling. *BMC Pharmacol. Toxicol.* **2012**, *13*, 3.

(17) Valant, C.; Sexton, P. M.; Christopoulos, A. Orthosteric/allosteric Bitopic Ligands: Going Hybrid at GPCRs. *Mol. Interv.* **2009**, *9*, 125–135.

(18) Valant, C.; Lane, J. R.; Sexton, P. M.; Christopoulos, A. The Best of Both Worlds? Bitopic Orthosteric/Allosteric Ligands of G Protein-Coupled Receptors. *Annu. Rev. Pharmacol. Toxicol.* **2012**, *52*, 153–178.

(19) Baltos, J.; Gregory, K. J.; White, P. J.; Sexton, P. M.; Christopoulos, A. Quantification of Adenosine A₁ Receptor Biased Agonism: Implications for Drug Discovery. *Biochem. Pharmacol.* **2016**, *99*, 101–112.

(20) Devine, S. M.; May, L. T.; Scammells, P. J. Design, Synthesis and Evaluation of N⁶-substituted 2-Aminoadenosine-5'-N-methylcarboxamides as A₃ Adenosine Receptor Agonists. *MedChemComm.* **2014**, *5*, 192–196.

(21) Devine, S. M.; Scammells, P. J. Synthesis and Utility of 2-Halo-O⁶-(benzotriazol-1-yl)-functionalized Purine Nucleosides. *Eur. J. Org. Chem.* **2011**, *6*, 1092–1098.

(22) Middleton, R. J.; Briddon, S. J.; Cordeaux, Y.; Yates, A. S.; Dale, C. L.; George, M. W.; Baker, J. G.; Hill, S. J.; Kellam, B. New Fluorescent Adenosine A₁-Receptor Agonists that Allow Quantification of Ligand-Receptor Interactions in Microdomains of Single Living Cells. *J. Med. Chem.* **2007**, *50*, 782–793.

(23) Valant, C.; Aurelio, L.; Devine, S. M.; Ashton, T. D.; White, J. M.; Sexton, P. M.; Christopoulos, A.; Scammells, P. J. Synthesis and Characterization of Novel 2-Amino-3-benzoylthiophene Derivatives as Biased Allosteric Agonists and Modulators of the Adenosine A₁ Receptor. *J. Med. Chem.* **2012**, *55*, 2367–2375.

(24) Aurelio, L.; Valant, C.; Flynn, B. L.; Sexton, P. M.; White, J. M.; Christopoulos, A.; Scammells, P. J. Effects of Conformational Restriction of 2-Amino-3-benzoylthiophenes on A₁ Adenosine Receptor Modulation. *J. Med. Chem.* **2010**, *53*, 6550–6559.

(25) Kenakin, T.; Watson, C.; Muniz-Medina, V.; Christopoulos, A.; Novick, S. A Simple Method for Quantifying Functional Selectivity and Agonist Bias. *ACS Chem. Neurosci.* **2012**, *3*, 193–203.

(26) Hutchinson, S. A.; Baker, S. P.; Scammells, P. J. N⁶-Disubstituted Adenosines: Potent and Selective A₁ Adenosine Receptor Agonists. *Bioorg. Med. Chem.* **2002**, *10*, 1115–1122.

(27) Ashton, T. D.; Baker, S. P.; Hutchinson, S. A.; Scammells, P. J. N⁶-Substituted C5'-Modified Adenosines as A₁ Adenosine Receptor Agonists. *Bioorg. Med. Chem.* **2008**, *16*, 1861–1873.

(28) Nguyen, A. T. N.; Baltos, J. A.; Thomas, T.; Nguyen, T. D.; Munoz, L. L.; Gregory, K. J.; White, P. J.; Sexton, P. M.; Christopoulos, A.; May, L. T. Extracellular Loop 2 of the Adenosine A₁ Receptor has a Key Role in Orthosteric Ligand Affinity and Agonist Efficacy. *Mol. Pharmacol.* **2016**, *90*, 703–714.

(29) Nguyen, A. T. N.; Vecchio, E. A.; Thomas, T.; Nguyen, T. D.; Aurelio, L.; Scammells, P. J.; White, P. J.; Sexton, P. M.; Gregory, K. J.; May, L. T.; Christopoulos, A. Role of the Second Extracellular Loop of the Adenosine A₁ Receptor on Allosteric Modulator Binding, Signaling, and Cooperativity. *Mol. Pharmacol.* **2016**, *90*, 715–725.

(30) Glukhova, A.; Thal, D. M.; Nguyen, A.T.N.; Vecchio, E. A.; Jörg, M.; Scammells, P. J.; May, L. T.; Sexton, P. M.; Christopoulos, A. Structure of the Adenosine A₁ Receptor Reveals the Basis for Subtype Selectivity. *Cell*, **2017**, *168*, 867–877.

(31) Vecchio, E.A.; Chuo, C. H.; Baltos, J.; Ford, L.; Scammells, P. J.; Wang, B. H.; Christopoulos, A.; White, P. J.; May, L. T.; The Hybrid Molecule, VCP746, is a Potent Adenosine A_{2B} Receptor Agonist that Stimulates Anti-fibrotic Signalling. *Biochem. Pharmacol.* **2016**, *117*, 46–56.

(32) Carpenter, B.; Nehme, R.; Warne, T.; Leslie, A. G. W.; Tate, C. G. Structure of the Adenosine A_{2A} Receptor Bound to an Engineered G Protein. *Nature*, **2016**, *536*, 104–107.

(33) Lebon, G.; Warne, T.; Edwards, P. C.; Bennett, K.; Langmead, C. J.; Leslie, A. G. W.; Tate, C. G. Agonist-bound Adenosine A_{2A} Receptor Structures Reveal Common Features of GPCR Activation, *Nature*, **2011**, *474*, 521–525.

(34) Bruns, R. F.; Fergus, J. H.; Coughenour, L. L.; Courtland, G. G.; Pugsley, T. A.; Dodd, J. H.; Tinney, F. J. Structure-activity Relationships for Enhancement of Adenosine A₁ Receptor binding by 2-Amino-3-benzoylthiophenes, *Mol. Pharmacol.* **1990**, *38*, 950–958.

(35) Stewart, G. D.; Valant, C.; Dowell, S.J.; Mijaljica, D.; Devenish, R.J.; Scammells, P.J.; Sexton, P. M.; Christopoulos, A. Determination of Adenosine A₁ Receptor Agonist and Antagonist Pharmacology using *Saccharomyces Cerevisiae*: Implications for Ligand Screening and Functional Selectivity, *J Pharmacol Exp Ther.* **2009**, *331*, 277–286.

(36) Baltos, J.; Vecchio, E. A.; Harris, M. A. Qin, C. X.; Ritchie, R. H. Christopoulos, A.; White, P. J. May, L. T. Capadenoson, a Clinically Trialed Partial Adenosine A₁ Receptor Agonist, can Stimulate A_{2B} Receptor Biased Agonism. *Biochem. Pharmacol.* **2017**, *135*, 79–89.

(37) Eswar, N.; Webb, B.; Marti-Renom, M. A.; Madhusudhan, M. S. Eramian, D.; Shen, M-Y.; Pieper, U.; Sali, A. Comparative Protein Structure Modeling using MODELLER. Comparative Protein Structure Modeling using MODELLER. *Current Protocols in Protein Science*, **2007**, chapter 2, unit 2.9.

(38) An, J.; Totrov, M.; Abagyan, R. Pocketome via Comprehensive Identification and Classification of Ligand Binding Envelopes. *Mol. Cell Proteomics*, **2005**, *4*, 752–761.

(39) Abagyan, R.; Kufareva, I. The Flexible Pocketome Engine for Structural Chemogenomics. *Methods Mol Biol*, **2009**, *575*, 249–279.

(40) Ballesteros, J. A.; Weinstein, H. Integrated Methods for the Construction of Three-Dimensional Models and Computational Probing of Structure-Function Relations in G Protein-Coupled Receptors, *Methods in Neurosciences*, **1995**, *25*, 366–428.

1
2
3
4
5
6
7
8
9
10
11
12
13
14
15
16
17
18
19
20
21
22
23
24
25
26
27
28
29
30
31
32
33
34
35
36
37
38
39
40
41
42
43
44
45
46
47
48
49
50
51
52
53
54
55
56
57
58
59
60

TABLE OF CONTENTS GRAPHIC

